AWARD NUMBER: W81XWH-14-1-0178

TITLE: Reprogramming of the Ovarian Tumor Stroma by Activation of a Biomechanical ECM Switch

PRINCIPAL INVESTIGATOR: Peter Brooks

CONTRACTING ORGANIZATION: Maine Medical Center
Portland, ME 04102

REPORT DATE: September 2016

TYPE OF REPORT: Final

PREPARED FOR: U.S. Army Medical Research and Materiel Command
Fort Detrick, Maryland 21702-5012

REPORT DOCUMENTATION PAGE

Form Approved
OMB No. 0704-0188

1. REPORT DATE	2. REPORT TYPE	3. DATES COVERED
September 2016	Final	15 Jul 2014 - 14 Jul 2016

4. TITLE AND SUBTITLE

Reprogramming of the Ovarian Tumor Stroma by Activation of a Biomechanical ECM Switch

5a. CONTRACT NUMBER

5b. GRANT NUMBER
W81XWH-14-1-0178

5c. PROGRAM ELEMENT NUMBER

6. AUTHOR(S)

Peter Brooks, PhD

E-Mail: brookp1@mmc.org

5d. PROJECT NUMBER

5e. TASK NUMBER

5f. WORK UNIT NUMBER

7. PERFORMING ORGANIZATION NAME(S) AND ADDRESS(ES)

Maine Medical Center
22 Bramhall Street
Portland, ME 04102-3134

8. PERFORMING ORGANIZATION REPORT NUMBER

9. SPONSORING / MONITORING AGENCY NAME(S) AND ADDRESS(ES)

U.S. Army Medical Research and Materiel Command
Fort Detrick, Maryland 21702-5012

10. SPONSOR/MONITOR'S ACRONYM(S)

11. SPONSOR/MONITOR'S REPORT NUMBER(S)

12. DISTRIBUTION / AVAILABILITY STATEMENT

Approved for Public Release; Distribution Unlimited

13. SUPPLEMENTARY NOTES

14. ABSTRACT

Abstract: Ovarian cancer is the most lethal form of gynecological malignancies with limited durable responses observed following front line treatment for late stage recurrent disease. We proposed to assess the role of alpha 10 beta 1 on tumor growth and chemosensitivity in vivo. We have made significant progress towards the completion of the overall goals of this project. In particular we, have characterized stromal cell infiltration of ovarian tumors and have shown extensive infiltration of tumor associated blood vessels as well as fibroblasts which can express high levels of pro-tumorigenic cytokines. Targeting the HU177 collagen epitope recognized by alpha 10 beta 1 significantly reduced angiogenesis and fibroblast infiltration. Interestingly, while reducing expression of alpha 10 beta 1 can inhibit fibroblast migration on denatured collagen; it failed to reduce cell adhesion. Moreover a peptide antagonist of alpha 10 beta 1 may inhibit ovarian tumor growth in vivo. Our studies suggest that the number and size of ovarian tumors was reduced in transgenic mice that lack alpha 10 beta 1 and a reduction in stromal cell infiltration was observed in tumors from alpha 10 beta 1 null mice. Moreover, our data suggest the presence of fibroblast that express integrin alpha 10 beta 1 may provide a growth advantage to ovarian tumors in vivo. Collectively, our new findings support the hypothesis that alpha 10 beta 1plays a role in regulating stromal cell behavior and ovarian tumor growth.

15. SUBJECT TERMS

Ovarian cancer □SMA Integrin alpha10 beta1 Stromal Fibroblast Angiogenesis Cisplatin Chemosensitivity Cell adhesion Cell migration Cell proliferation Cytokines

16. SECURITY CLASSIFICATION OF:			17. LIMITATION OF ABSTRACT	18. NUMBER OF PAGES	19a. NAME OF RESPONSIBLE PERSON
a. REPORT	b. ABSTRACT	c. THIS PAGE			USAMRMC
Unclassified	Unclassified	Unclassified	Unclassified	30	19b. TELEPHONE NUMBER *(include area code)*

Table of Contents

Page

Introduction: Ovarian cancer continues to represent one of the most lethal forms of malignancies among women. While chemotherapy has demonstrated some level of efficacy, recurrent tumors often exhibit a significant level of chemoresistance with limited efficacy observed with second and third line therapies. In addition to the malignant ovarian tumor cells themselves, stromal infiltrates such as cancer-associated fibroblasts (CAFs) represent a major component of malignant ovarian tumors. Accumulating evidence indicates that stromal cell infiltrates may play an important role in regulating tumor growth as well as chemoresistance. However, the mechanisms that control stromal cell infiltration into ovarian tumor are not completely understood. Interestingly, biochemical experiments and biophysical studies have demonstrated extensive collagen remodeling in ovarian tumor as compared to normal tissues. This differential ECM configuration might provide a unique means for selectively regulating stromal cell behavior since interactions with remodeled ECM may alter cell adhesion, migration, proliferation, survival and gene expression. To this end, the overall goal of this proposal was to test the hypothesis that alterations of the biophysical structure of collagen results in the exposure of a previously unrecognized alpha 10 beta 1 integrin-binding element that facilitates reprogramming and accumulation of a subset of host derived CAF-like stromal cells that support tumor growth and modulate chemosensitivity. In this regard, we proposed two specific aims for this pilot project. The first aim was to assess the role of alpha 10 beta 1 on tumor growth and chemosensitivity in vivo using murine and human ovarian tumor models. We examined the impact of function blocking antagonists directed to alpha 10 beta 1 alone and in combination with chemotherapy on ovarian tumor growth in vivo. In the second aim, we examined and characterize cellular and molecular mechanisms by which alpha 10 beta 1 expressed in the stromal cells modulates tumor growth and chemosensitivity.

2). Key Words:
1). Ovarian cancer
2). Alpha SMA
3). Integrin alpha 10 beta 1
4). Stromal Fibroblast
5). Angiogenesis
6). Cisplatin
7). Chemosensitivity
8). Cell adhesion
9). Cell migration
10). Cell proliferation
11). Cytokines

3). Accomplishments:
Summary of major goals of the project:
A). As outlined in aim 1 (tasks 1-3) we proposed to analyze the effects of antagonists of alpha 10 beta 1 alone and in combination with chemotherapy on tumor growth in vivo using both transgenic and wild type human and murine ovarian tumor models. We carried out a histopathological analysis of the ovarian tumors along with an analysis of potential changes in cytokine expression in both serum and conditioned medium from stromal cells.

B). As outlined in aim 1 (task 4) we proposed to analyze the growth of ovarian cancer cells mixed with alpha 10 beta 1 fibroblast variants in mice alone and in combination with chemotherapy. We carry out a histopathological analysis of the ovarian tumors along with an analysis of changes in cytokine expression in both serum and conditioned medium from stromal cells.

C). As outlined in aim 2 (tasks 1 and 2) we analyzed the role of alpha 10 beta 1 in regulating stromal cell adhesion, migration and proliferation on distinct ECM substrates including native and denatured collagen.

D). As outlined in aim 2 (task 3) we analyzed the role of alpha 10 beta 1 on fibroblast growth factors and cytokines and their impact on ovarian tumor cell behavior.

Specific Accomplishments for reporting period as they relate to the major goals described above.
We have made significant progress towards the overall goals of our project (July 2014 through July 2016). In this regard, we have detailed all the completed experiments to date and summarized the overall accomplishments and experimental results achieved during the project below. In addition, studies outlined in this project were also used as part of a manuscript that was published (see appendix). A detailed summary of the research accomplishments as they pertain to the tasks outlined in the statement of work is provided below.

Tumorigenic properties and stromal infiltration of murine ID8 and human SKOV-3 ovarian tumors in in vivo. Our studies suggested that targeting the HU177 cryptic epitope recognized by integrin alpha 10 beta 1 inhibited SKOV-3 tumor growth in vivo and reduced the accumulation of alpha SMA expressing stromal cells by approximately 70% (See Appendix). To further examine changes in stromal infiltration of ovarian tumors as outlined in aim 1, we quantifying basal levels of angiogenesis in SKOV-3 tumors as well as the levels of angiogenesis following treatment with antagonists of the HU177 collagen epitope. As shown in figure 1A and B, mice carrying SKOV-3 tumors exhibited an approximately 35% reduction in angiogenesis as compared to controls. Next we began to establish the working conditions to assess the growth properties of murine ID8 ovarian tumors in C57BL/6 mice. Briefly, ID8 cells ($5x10^6$) were injected subcutaneously into C57BL/6 mice and resulting tumors were analyzed 6 weeks later. As shown in figure 1C, small be definable ID8 ovarian tumors formed as indicated by H&E staining. While solid tumor did form, the resulting tumors were very small and thus a much larger number of tumor cells as well as a longer incubation period were needed to establish larger tumors for a more accurate analysis. Finally, to assess whether alpha SMA expressing stromal cells are able to infiltrate these early stage ID8 tumors, frozen sections were prepared and stained for the presence of alpha SMA expressing stromal cells. As shown in figure 1D, alpha SMA expressing stromal cell were readily detected within these ID8 ovarian carcinomas.

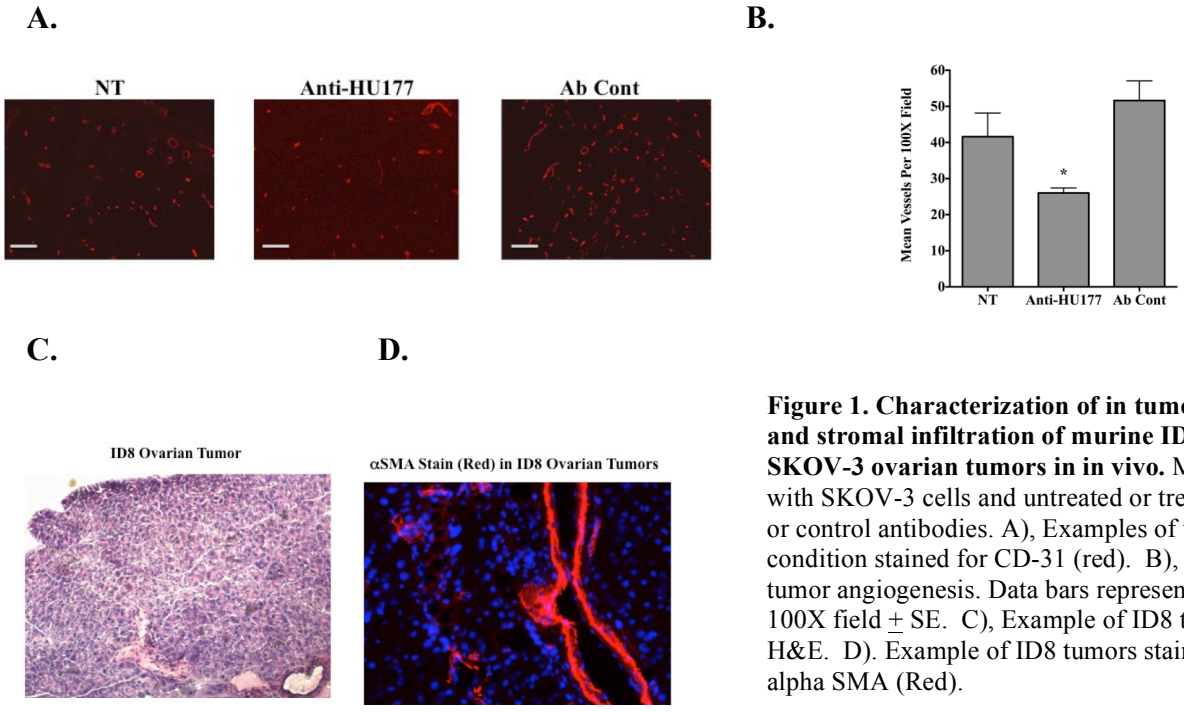

Figure 1. Characterization of in tumorigenic properties and stromal infiltration of murine ID8 and human SKOV-3 ovarian tumors in in vivo. Mice were injected with SKOV-3 cells and untreated or treated with anti-HU177 or control antibodies. A), Examples of tumors from each condition stained for CD-31 (red). B), Quantification of tumor angiogenesis. Data bars represent mean vessels per 100X field $\pm$ SE. C), Example of ID8 tumors stained by H&E. D). Example of ID8 tumors stained for expression of alpha SMA (Red).

Analysis of stromal infiltration of murine ID8 ovarian tumors in in vivo. Recent studies have indicated immune suppression in ovarian cancer may govern the efficacy of current therapies. Given our data, we extended our studies to examine the levels and distribution of the immune checkpoint molecule PD-L1 in ID8 tumors. Interestingly, while minimal levels PD-L1 (Red) was detected in association with tumor cells or CD8+ T-cells (green), PD-L1 appeared to be more strongly associated with stromal infiltrates (fig 2A). To confirm these observations we stained the tumors for PD-L1 and alpha SMA. PD-L1 was extensively associated with alpha SMA positive CAF-like cells (fig 2B). These results indicate that alpha SMA expressing CAF-like stromal cells express considerable levels of PD-L1 and may contribute to immune suppression in these ID8 tumors.

A.

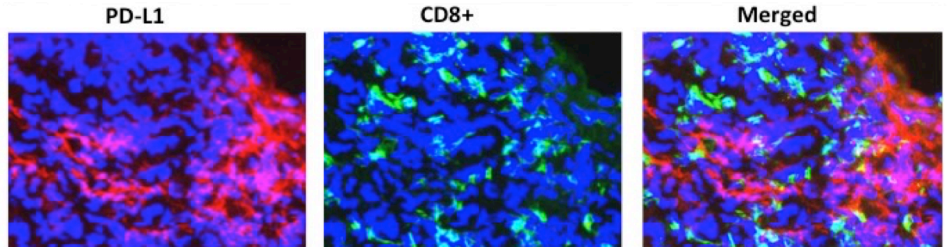

B.

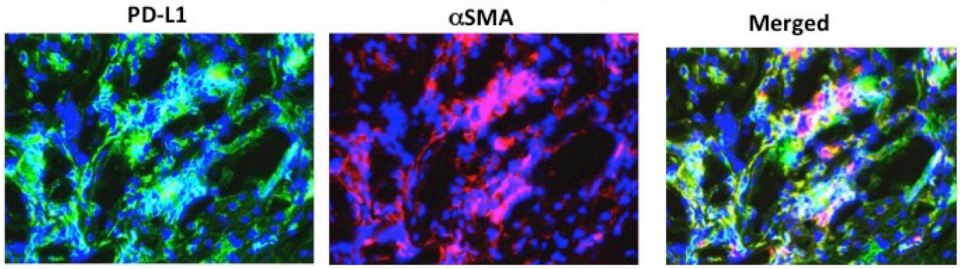

Figure 2. Expression of PD-L1, CD8 and alpha SMA in ID8 tumors. ID8 tumor cells were injected into C57BL/6 mice. A). PD-L1 (red) and CD8+ T-cells (green) in ID8 ovarian tumors. B). PD-L1 (green) and alpha SMA (red) in ID8 ovarian tumors.

Effects of PGF peptide on alpha 10 beta 1 integrin binding to denatured collagen. Our studies suggested that integrin alpha 10 beta 1 directly binds the PGF peptide, which contains critical residues within the HU177 cryptic collagen epitope. To examine the ability of the synthetic PGF collagen peptide to act as an antagonist of alpha 10 beta 1 integrin we assessed the ability of the PGF peptide to reduce binding of recombinant alpha 10 beta 1 to denatured collagen in a competition ELISA. As shown in figure 3, incubation of the PGF-peptide, but not a control non-specific peptide with recombinant alpha 10 beta 1 reduced it's binding by approximately 60% as compared with control. These findings are consistent with our previous studies indicating that the Mab directed to the HU177 collagen epitope inhibited alpha 10 beta 1 binding to denatured collagen by 60% and suggest that the PGF-peptide inhibits alpha 10 beta 1 binding at the concentrations tested.

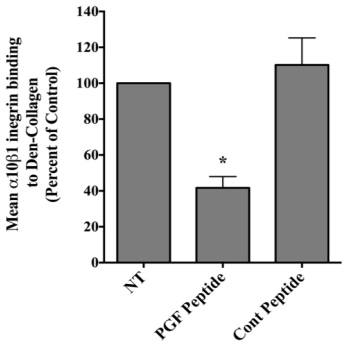

Figure 3. Effects of PGF peptide on alpha 10 beta 1 **integrin binding to denatured collagen.** Integrin alpha 10 beta 1 binding to denatured collagen in the presence of synthetic HU177 epitope or control peptide. Data bars represent mean integrin binding indicated as percent of control± SE from 3 experiments. * P<0.05 as compared to controls.

The co-inhibitory molecule PD-L1 is expressed in alpha SMA expressing CAF-like cells and closely associates with the HU177 collagen epitope in ID8 tumors. Our studies (see Appendix) indicate that alpha SMA positive stromal cells are closely associated with the HU177 epitope in ovarian tumors. Moreover, the expression of PD-L1 in the ID8 ovarian tumors appeared to co-localize with stromal infiltrates rather than

CD8+ T-cells. Therefore, we co-stained ID8 tumors for HU177 epitope and PD-L1. PD-L1 positive cells (green) closely associated (yellow) with the HU177 (red) epitope (fig 4A). To examine whether PD-L1 was also expressed in alpha SMA positive fibroblasts that express markers of an activated or CAF-like phenotype, we analyzed lysates from, transformed NIH-3T3 and rat fibroblasts, and isolated CAFs. Fibroblasts exhibiting CAF-like phenotype express PD-L1 (fig 4B). Given these studies, PD-L1 expressed within the stromal compartment may lead to immune suppression as a result of selective interactions between PD-L1 expressed on the CAF-like fibroblasts and PD-1 expressing T-cells entering the tumors thereby resulting in reduced T-cell cytotoxic functions ultimately resulting in reduced overall immune control of these ovarian tumors.

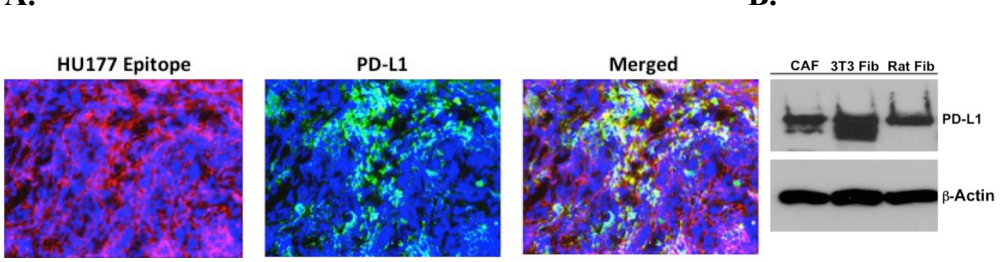

Figure 4. Expression of HU177 epitope, and PD-L1 in ID8 tumor and levels of PD-L1 in CAF-like cells. A). Examples of HU177 epitope (red) and PD-L1 (green) in ID8 ovarian tumors. B). Western blot of lysates from CAFs, immortalized 3T3 and rat fibroblasts for PD-L1.

The HU177 collagen epitope can support T-cell interactions but antagonists to this epitope failed to block T-cell adhesion in vitro. Next, given our observations, we examined the ability of T-cell lines to bind denatured collagen, and examined whether the HU177 epitope played a role in this adhesive event in vitro. Surprisingly, while T-cell lines expressed alpha 10 integrin, one of at least two integrins capable of binding to the HU177 epitope (fig 5A), anti-HU177 antibody failed to block T-cell adhesion to denatured collagen (fig 5B). These data suggest that the HU177 collagen epitope may not play a direct role in mediating T-cell adhesion under these conditions.

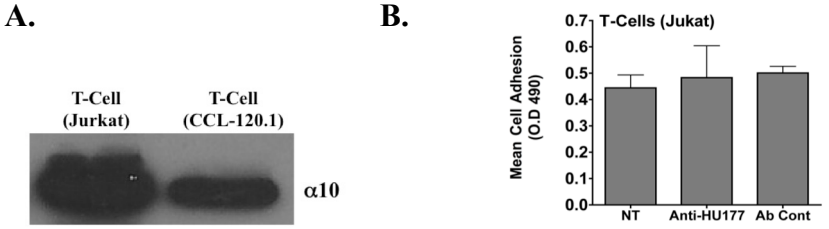

Figure 5. Anti-HU177 antibody failed to inhibit T-cell adhesion even though they express alpha 10 integrin. A). Analysis of T-cell lines for alpha 10 integrin by western blot. B). Quantification of T-cell adhesion to denatured collagen. Data bars represent mean cell adhesion ± S.E from triplicate wells.

Conditioned medium (CM) from human fibroblast (HF) that exhibit a CAF-like phenotype stimulate elevated levels of PD-L1 in T-cells. Our studies indicate a functional role for CAF-like cells in regulating ovarian tumor growth and cellular interactions with the HU177 collagen epitope regulate stromal cell infiltration into ovarian tumors. Studies have documented that CAF-like stromal cells contribute to immune suppression and may regulate T-cell functions. Given that blocking the HU177 epitope in vivo reduced CAF-like stromal cell infiltration into ovarian tumors, we sought to examine the effects conditioned medium (CM) from CAF-like fibroblasts might have on immune checkpoint molecule PD-L1 within T-cells. Incubation of T-cells with fibroblast CM increased expression of PD-L1 (fig 6). These findings suggest that soluble factors released from these CAF-like cells may contribute to immune suppression by stimulating enhanced levels of PD-L1. Thus, it is possible that blocking infiltration of CAF-like stromal cells within ovarian tumors with anti-HU177 antibody may limit and/or reverse immune suppression associated with ovarian cancer.

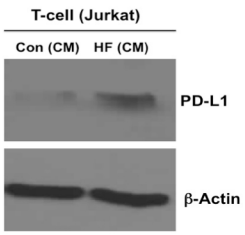

Figure 6. Conditioned medium (CM) from human fibroblast (HF) that exhibit a CAF-like phenotype stimulate elevated levels of PD-L1 in T-cells. Human fibroblasts that exhibit a CAF-like phenotype (express alpha SMA, PDGFR alpha and activated NFkb) were used to prepare serum free concentrated 10X (HF CM) or 10X serum free medium without cells (Con CM). CM was used to stimulate T-cells for 24rs and whole cell lysates prepared. Lysates from T-cell stimulated with HF conditioned medium (CM) was analyzed for the expression of PD-L1 by western blot.

Stimulation of T-cells with soluble HU177 collagen epitope peptide (PGF-peptide) alters protein expression. Significantly higher levels of a soluble circulating form of the HU177 epitope has been documented in human subjects with melanoma as compared to control subjects, and the levels of this soluble HU177 epitope correlated with tumor thickness, recurrence and death. Thus, soluble HU177 collagen epitope may facilitate tumor progression. To this end we, examined the effects of the soluble HU177 collagen epitope PGF-peptide (CPGFPGFC) on PD-L1 expressed in T-cells. Stimulation of T-cells with the soluble HU177 epitope resulted in minimal changes in PD-L1 (fig 7A). Surprisingly, stimulation of T-cells with the HU177 epitope dramatically enhanced the levels of Bcl11b (Fig 7B), a zinc finger T-cell transcription factor that regulates T-cell functions. Importantly, Bcl11b plays critical roles in the immune suppressive activity of T-Regs. Moreover, studies indicate that reducing levels of Bcl11b in T-cells subsets leads to reprograming of T-cells into natural killer (NK)-like cells called ITNK cells that express high levels of perforin, granzyme B, and INF-gamma, which collectively control the ability of NK cells to kill tumors. Therefore, it is possible that targeting the HU177 collagen epitope with anti-HU177 antibody, may not only reduce immune suppressive CAF-like stromal infiltration, but may also contribute to the reversal of immune suppression by blocking the ability of the soluble HU177 epitope from inducing Bcl11b expression in T-cells thereby reducing T-Reg functions and enhancing the formation of NK-like cells.

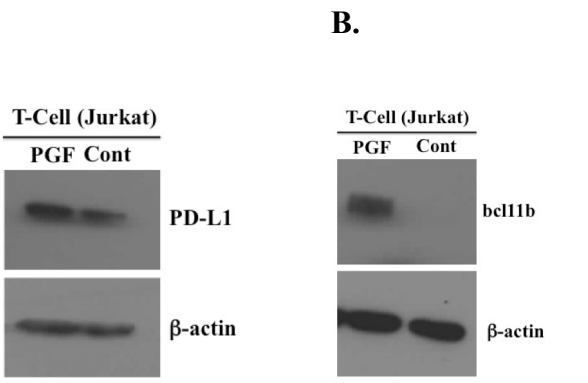

Figure 7. Stimulation of T-cells with soluble HU177 collagen epitope peptide (PGF-peptide) alters protein expression. Jurkat T-cells were incubated (100ng/ml) with soluble HU177 collagen epitope peptide (CPGFPGFC) or control peptide (CQGPSGAPGEC) and whole cell lysates prepared. A). Analysis of T-cell lysates for expression of PD-L1 by western blot. B). Analysis of T-cell lysates for expression of Bcl11b by western blot.

Effects of PGF peptide on fibroblast cell adhesion and migration. Given our studies indicating the ability of the PGF peptide to inhibit alpha 10 beta 1 -binding activity, we next examined the ability of this peptide to alter fibroblast cell adhesion and migration on denatured collagen. As shown in figure 8A, incubation of alpha SMA expressing fibroblasts with the PGF collagen peptide resulted in a significant ($P<0.05$) approximately 50% inhibition of adhesion to denatured collagen. In similar studies the PGF-peptide also significantly ($P<0.05$) inhibited fibroblast migration by approximately 50% (Figure 8B). Collectively these important findings confirm the function blocking ability of the PGF-peptide to disrupt fibroblast adhesion and migration on denatured collagen.

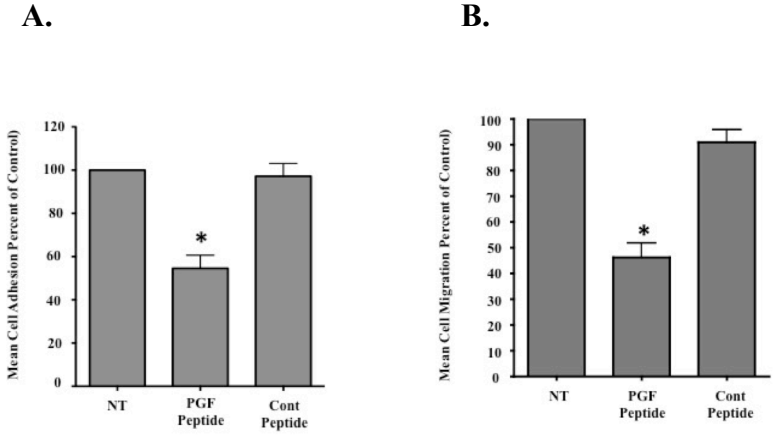

Figure 8. Effects of PGF peptide on fibroblast adhesion and migration on denatured collagen. Human fibroblasts were resuspended in the presence or absence the HU177 cryptic collagen epitope peptide (PGF) or control peptide. A). Data bars represent mean adhesion indicated as percent of control± SE from 3 experiments. B). Data bars represent mean migration indicated as percent of control± SE from 3 experiments. * $P<0.05$ as compared to controls.

Effects of antagonists of alpha 10 beta 1 alone and in combination with cisplatin on ovarian tumor growth in vivo. As outlined in specific aim 1, we assess the effects of combining cisplatin with antagonists of the alpha 10 beta 1. Nude mice were first injected with SKOV-3 human ovarian tumor cells and 3 days later were treated with control DMSO, or anti- alpha 10 beta 1 peptide (PGF) alone, cisplatin alone or a combination of both. Tumor size was monitored by caliper measurements for 21 days. As shown in figure 9, cisplatin (10.0mg/Kg), which was given twice per-week, inhibited SKOV-3 tumor growth. Interestingly, similar inhibition of tumor growth was initially observed with anti- alpha 10 beta 1 peptide PGF (10.0mg/Kg) given three times per week within the first 2 weeks, however, by 21 days the relative inhibition of tumor growth was less. Surprisingly, while no additive or synergistic effects were observed following combining cisplatin and the PGF peptide (10.0mg/Kg), these preliminary studies suggest that targeting the alpha 10 beta 1 in SKOV-3 tumors may represent a novel strategy to regulate the growth of ovarian tumors in vivo. Additional experiments using a range of concentrations will be required to determine whether combining PGF-peptide may enhance the anti-tumor activity of cisplatin. Given the limited anti-tumor activity observed at later time points, additional studies are underway to examine whether alterations in concentrations over time may result in the PGF-peptide acting as an agonists instead of an antagonist.

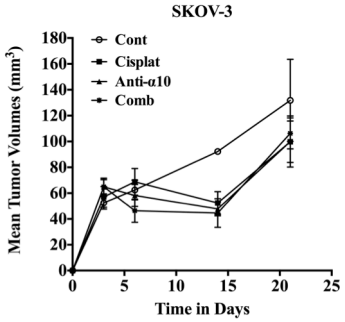

Figure 9. Effects of antagonists of alpha 10 beta 1 alone and in combination with cisplatin on ovarian tumor growth in vivo. Human SKOV-3 ovarian carcinoma cells ($3x10^6$/mouse) were injected in nude mice. Three days later mice were treated i.p with vehicle control (DMSO), cisplatin (10mg/kg) alone, anti- alpha 10 beta 1 peptide PGF (10.0mg/kg) alone or a combination of both. Data bars represent mean tumor volumes $\pm$ standard errors from 6 mice per condition.

Histopathological analysis of tumors treated with antagonists of alpha 10 beta 1 alone and in combination with cisplatin. As outlined in specific aim 1, we began to establish the working conditions for immunohistological quantification of cancer associated stromal cells including alpha SMA expressing fibroblasts infiltrates. As shown in figure 10 alpha SMA expressing stromal cells (red) were readily detected in control treated SKOV-3 tumors at the 21-day time point. Interestingly, a reduction in the relative levels of alpha SMA expressing stromal cells was observed in tumors in what appeared to be a distinct subset of cells as some isolated alpha SMA expressing cells still remained as small isolated groups scattered throughout the tumor. While quantification is clearly required, initial observations also suggest that cisplatin had little effect on the infiltration of alpha SMA expressing cells. In fact, slightly enhanced levels were observed in these tumors as compared to controls, while tumors from the combination treated mice had a similar distribution of alpha SMA as was observed with tumors treated with PGF peptide alone.

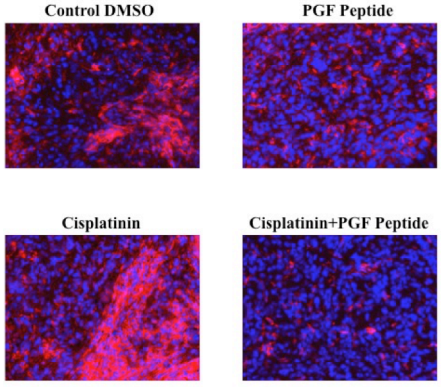

Figure 10. Histopathological analysis of tumors treated with antagonists of alpha 10 beta 1 alone and in combination with cisplatin SKOV-3 ovarian carcinoma cells ($3x10^6$/mouse) were injected in nude mice. Three days later mice were treated i.p with vehicle control (DMSO), cisplatin (10mg/kg) alone, anti-alpha 10 beta 1 peptide PGF (10.0mg/kg) alone or a combination of both. Frozen sections from each tumor were stained for expression of alpha SMA (Red). Photos (200x) represent examples from each experimental condition.

Analysis of serum samples from mice treated with antagonists of alpha 10 beta 1 alone and in combination with cisplatin. Given the surprising findings that treatment of mice bearing SKOV-3 ovarian tumors with the PGF-peptide had only minimal effect at later time points, we carried out preliminary study to establish the conditions to examine serum from these treated mice for a panel of inflammatory cytokines. As shown in figure 11, after the relative cytokine levels were corrected for non-specific signal treatment of mice with the PGF-peptide caused a dramatic increase in the detectable levels of TGFb1 in the serum as compared to control (DMSO) treated mice. Similar results were obtained from a second mouse. Interestingly, cisplatin treatment also caused an increase in TGFb1. Little if any detection of the other cytokines was observed in the serum under these specific conditions, possibly do to the dilution of serum. Additional experiment will be required to confirm these results.

Cytokine	Positive Control	DMSO-treated	PGF-treated	Cispl-treated	Combin-treated
MIP-1b	4.000	0.000	0.000	0.000	0.010
MIP-1a	3.821	0.000	0.000	0.000	0.042
MCP-1	3.767	0.007	0.020	0.098	0.513
TGFb1	3.797	0.008	0.389	0.205	0.388
IL-10	1.745	0.066	0.000	0.000	0.000
IL-6	2.762	0.071	0.000	0.000	0.016
IL-4	2.997	0.050	0.000	0.000	0.000
IL-1b	1.448	0.085	0.000	0.000	0.000
TNF-a	3.722	0.073	0.000	0.000	0.000
INF-g	1.872	0.099	0.000	0.000	0.000
IL-17a	3.634	0.082	0.000	0.000	0.000
IL-12	3.623	0.068	0.000	0.000	0.026

Figure 11. Analysis of serum samples from mice treated with antagonists of alpha 10 beta 1 alone and in combination with Cisplatin. Representative example of the relative detection of a panel of cytokines in serum from a mouse treated as indicated. Values indicate relative O.D (450nm) after subtraction for non-specific binding. ELISA detection of cytokines from a Multi-Analyte array kit.

Effects of alpha 10 beta 1 in alpha SMA expressing fibroblasts on collagen adhesion. As outlined in aim 2, we sought to examine the effects of alpha 10 beta 1 expression in fibroblast may have on cell adhesion. To examine the functional significance of alpha 10 beta 1 on fibroblasts adhesion, we first knocked down expression of α10 integrin by shRNA. To confirm efficient knock down of alpha 10 integrin whole cell lysates were prepared from fibroblasts transfected with shRNA directed to alpha 10 integrin (alpha 10-KD-HF) or a non-specific control (Con-KD-HF). As shown in figure 12A, little if any alpha 10 integrin was detected in alpha 10-KD-HF fibroblasts following western blot analysis. In contrast alpha 10 integrin was readily detected in wild type and control transfected fibroblasts. Next we examined the fibroblast cell variants for their ability to attach to defined ECM substrates. Surprisingly, while the parental wild-type fibroblasts (WT) and control transfected cells (Con-K/D) readily attached to either intact native collagen (Figure 12B) or denatured collagen (Figure 11C), fibroblasts in which alpha 10 integrin was knocked down exhibited enhanced adhesion. Addition experiments will be needed to confirm the significance of these surprising findings.

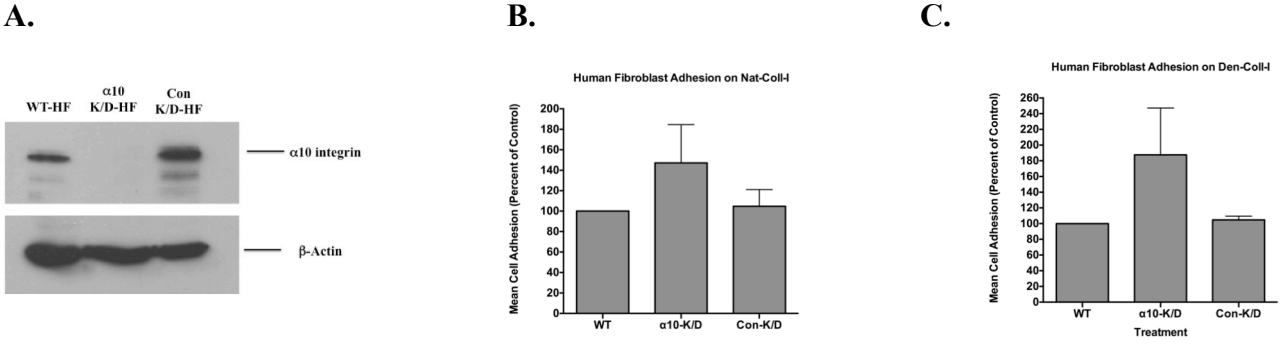

Figure 12. Effects of alpha 10 beta 1 in alpha SMA expressing fibroblasts on collagen adhesion. A). Wild type fibroblasts (WT-HF) were transfected with alpha 10-integrin shRNA (alpha 10K/D-HF) or non-specific control (ConK/D-HF). Western blot analysis indicates reduction of alpha 10 integrin in alpha 10 integrin (alpha 10K/D-HF) cells. B). Quantification of fibroblasts variants attachment to native intact collagen. C). Quantification of fibroblasts variants attachment to denatured collagen. Data bars represent mean cell adhesion expressed as percent of control ± standard deviations from triplicate

Effects of alpha 10 integrin in alpha SMA expressing fibroblasts on collagen migration. As outlined in aim 2, we sought to examine the effects of alpha 10 beta 1 integrin expression in fibroblast may have on cell migration. Fibroblast cell variants described above were allowed to migrate using transwell migration chambers coated with denatured collagen. As shown in figure 13, while the parental wild-type fibroblasts (WT) and control transfected cells (Con-K/D) readily migrated on denatured collagen, fibroblasts in which alpha 10 integrin was knocked down exhibited significantly ($P<0.05$) reduced migration.

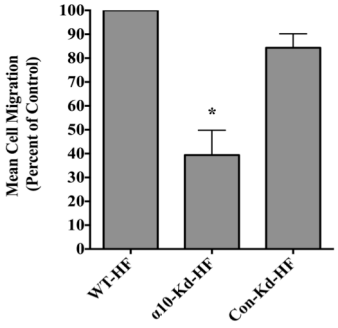

Figure 13. Effects of alpha 10 beta 1 in alpha SMA expressing fibroblasts on collagen migration. Integrin alpha 10 beta 1 expressing variants of human fibroblasts were seeded transwell membranes coated with denatured collagen and allowed to migrate for 2 hrs. Data bars represent mean cell migration indicated as percent of control from triplicate experiments. * $P<0.05$ as compared to controls.

Effects of alpha 10 beta 1 in alpha SMA expressing fibroblasts on proliferation. As outlined in aim 2, we sought to examine the effects of alpha 10 beta 1 expression in fibroblast may have on cell proliferation. To examine the functional significance of alpha 10 beta 1 on fibroblasts proliferation, fibroblast cell variants described above were allowed to proliferate for 24hrs on non-coated (Figure 14A), native collagen coated (Figure 14B), or denatured collagen coated micro-titer wells (Figure 14C). As shown in figure 8A-C, little if any change was observed in proliferation between control and alpha 10 knock down cells among the different ECM substrate conditions. These data are consistent with notion that integrin alpha 10 may play little if any direct role in fibroblasts proliferation under these experimental conditions.

A. **B.** **C.**

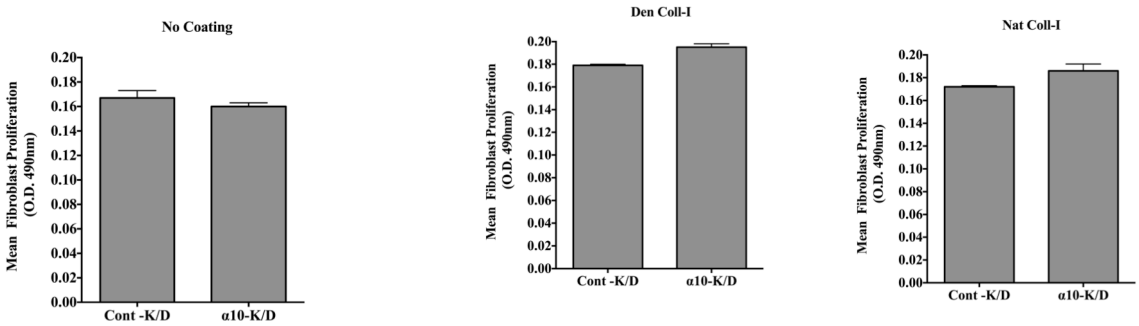

Figure 14. Effects of alpha 10 beta 1 in alpha SMA expressing fibroblasts on proliferation. Integrin alpha 10 beta 1 expressing fibroblasts variants were resuspended in proliferation buffer and seeded on microtiter wells that were either un-coated or coated with native collagen (Nat-Coll) or denatured collagen (Den-Coll). A). Quantification of cell proliferation on uncoated wells $\pm$ standard deviation from triplicate wells. B). Quantification of cell proliferation on native collagen coated wells $\pm$ standard deviation from triplicate wells. C). Quantification of cell proliferation on denatured collagen coated wells $\pm$ standard deviation from triplicate wells.

Effects of differential expression of alpha 10 beta 1 in fibroblasts on SKOV-3 tumor growth in vivo. Our studies indicate that knocking down expression of alpha 10 beta 1 in fibroblast had little if any direct effect of fibroblast proliferation in vitro (figure 14). However, reducing expression of alpha 10 beta 1 significantly reduced fibroblast migration. Given that integrin signaling can impact expression of a variety of secreted molecules that may impact growth of tumor cells, we examined the effects of fibroblasts with varying levels of alpha 10 beta 1 integrin might have on ovarian tumor growth in vivo. Briefly, nude mice (N=10 per condition) were injected with SKOV-3 tumor cells alone, or with SKOV-3 tumors mixed (4:1 ratio of tumor cells to fibroblast variants) with control transfect fibroblast (Cont-HF) or Fibroblasts in which the levels of alpha 10

integrin was reduced by transfection of alpha 10 specific shRNA (alpha 10K/O HF). Tumors were allowed to grow for 21 days. As shown in figure 15, SKOV-3 tumors in the presence of control-transfected alpha 10 beta 1 expressing fibroblasts were significantly larger than SKOV-3 tumor in the absence of exogenously added fibroblasts. Importantly, no significant change in the size was observed between tumors formed following injection of SKOV-3 cells alone and SKOV-3 cells mixed with a10K/O-HF. These studies suggest that while the absence of alpha10 integrin in the fibroblasts does not significantly impact the growth of the fibroblast in vitro, the absence of alpha 10 integrin in fibroblasts may impact the ability of fibroblasts to enhance SKOV-3 ovarian tumor growth in vivo.

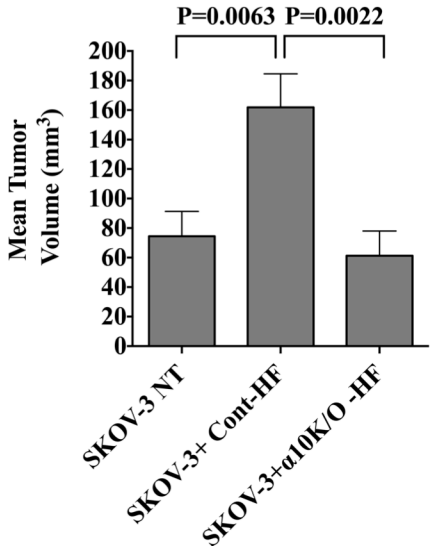

Figure 15. Effects of differential expression of alpha 10 beta 1 in fibroblasts on SKOV-3 tumor growth in vivo. SKOV-3 human ovarian tumor cells ($3x10^6$) alone or mixed with either control non-specific shRNA transfected human fibroblasts (Cont HF) or alpha 10 integrin specific shRNA transfected (alpha 10K/O-HF) fibroblasts at a tumor cell to fibroblast ratio 4:1 were injected subcutaneously. Quantification of mean SKOV-3 tumor volume from each experimental condition. Data bars represent mean tumor volume ± SE from 10 mice per condition.

Effects of conditioned medium from alpha SMA positive alpha 10 beta 1 expressing fibroblasts on SKOV-3 tumor cell proliferation. As outlined in specific aim 2, we sought to examine the possible role of soluble growth factors and cytokines present in conditioned medium of alpha 10 beta 1 expressing fibroblasts on ovarian tumor cell growth. To begin these studies, we first examined the ability of concentrated serum free conditioned medium (CM) from alpha 10 beta 1 expressing fibroblasts to impact SKOV-3 ovarian tumor cell growth in vitro. As shown in figure 16A, addition of CM from alpha 10 beta 1 expressing fibroblasts to SKOV-3 ovarian tumor cells significantly ($P<0.05$) enhanced proliferation as compared to control CM prepared in the absence of the fibroblasts. To confirm the ability of fibroblast CM to enhance SKOV-3 cell growth we examined the relative levels of KI67 antigen levels between un-stimulated and CM stimulated SKOV-3 cells by western blot. As shown in figure 16B, enhanced levels of KI67 were detected in lysate from fibroblast CM stimulated SKOV-3 cell as compared to control. Taken together these findings are consistent with the presence of soluble factors within the CM from these fibroblasts to promote SKOV-3 ovarian tumor cell growth.

A. B.

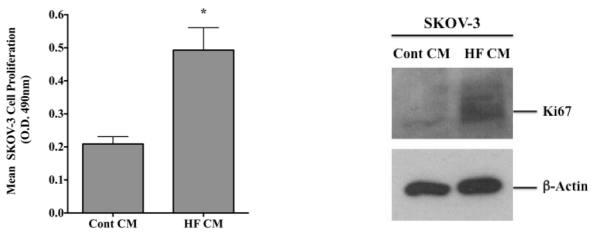

Figure 16. Effects of conditioned medium from alpha SMA positive alpha 10 beta 1 expressing fibroblasts on SKOV-3 tumor cell proliferation. A). SKOV-3 ovarian carcinoma cells were resuspended in the presence of serum free concentrated fibroblast conditioned medium (HF-CM) or concentrated medium prepared in the absence of fibroblasts (Cont-CM). SKOV-3 cells were allowed to proliferation for 24 hours. Data bars represent mean cell proliferation) ± standard deviations from triplicate wells. B). Western blot of whole cell lysates from SKOV-3 cells stimulated for 24 hours with Cont-CM or HF-CM and the levels of Ki67 antigen examined.

Effects of conditioned medium from alpha SMA positive alpha 10 beta 1 expressing fibroblasts on SKOV-3 tumor cell adhesion. As outlined in aim 2, we studied the effects of conditioned medium from alpha 10 beta 1 expressing fibroblasts variants might have of ovarian tumor cell. Briefly, 48-well non-tissue culture plates were coated with either intact (native) collagen or thermally denatured collagen. SKOV-3 tumor cells were resuspended in the presence or absence of 20ul of 10X conditioned medium (CM) and adhesion buffer and allowed to attach to the coated wells. As shown in figure 17A, CM derived from either control transfected fibroblasts or alpha 10 knock out fibroblasts had little if any effects on SKOV-3 cell adhesion to intact collagen. Similar experiments were carried out on denatured collagen. As shown in figure 17B, only a slight inhibition of SKOV-3 cell adhesion was detected in the presence of CM from alpha 10 knock out cells. Further studies will be required to determine whether enhanced inhibition can be observed in the presence of larger amounts of CM.

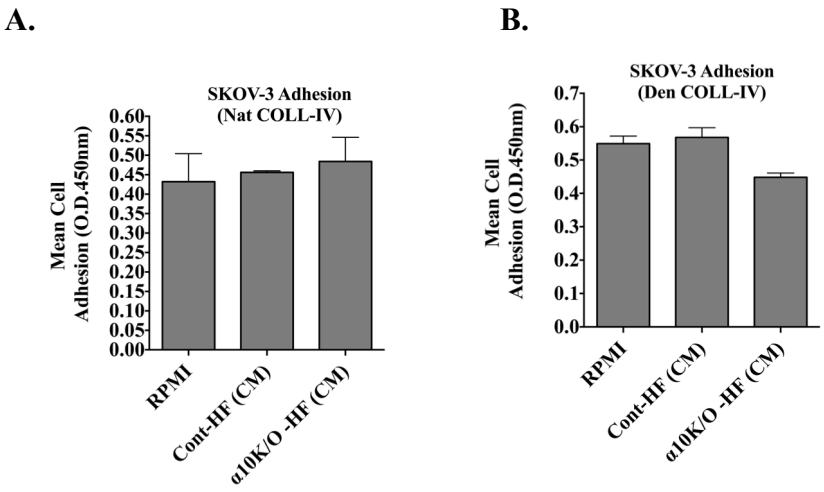

Figure 17. Effects of conditioned medium from alpha SMA positive alpha 10 beta 1 expressing fibroblasts on SKOV-3 tumor cell adhesion. SKOV-3 tumor cells were resuspended in the presence or absence the 20ul of 10X concentrated serum free conditioned medium from either control shRNA transfected or alpha 10 integrin specific shRNA transfected human fibroblasts. A). Data bars represent mean SKOV-3 cell adhesion to native collagen ± SE from triplicate wells. B). Data bars represent mean SKOV-3 cell adhesion to denatured collagen ± SE from triplicate wells.

Cytokine profile of alpha SMA positive alpha 10 beta 1 expressing fibroblasts. As outlined in specific aim 2, we sought to examine the possible role of alpha 10 beta 1 integrin binding to the HU177 cryptic epitope in modulating the expression of cytokines that may regulate ovarian tumor growth. Given the effects concentrated serum free CM on SKOV-3 growth in vitro, we next sought to establish a basal cytokine expression profile in alpha 10 beta 1 expressing fibroblasts under basal culture conditions. To begin these studies, 24 hour concentrated serum free CM) was collected and analyzed for the expression of multiple cytokines using a Multi-Analyte ELISA assay kit. As shown in figure 18, an array of cytokines thought to modulate ovarian tumor cell growth and stromal cell infiltration were differentially expressed. These data are consistent with the ability of fibroblasts conditioned medium to alter the growth properties of the SKOV-3 ovarian carcinoma cells described above.

Cytokine	Positive Control	FB CM	Negative Control
IL-1α	1.857	0.471	0.058
IL-1β	2.607	0.491	0.068
IL-2	0.707	0.759	0.066
IL-4	1.448	0.692	0.062
IL-6	0.606	1.554	0.052
IL-8	3.292	3.785	0.043
IL-10	1.440	0.678	0.043
IL-12	1.780	0.877	0.053
IL-17A	1.670	2.747	0.053
TNF-α	0.564	0.435	0.040
INF-γ	1.089	1.490	0.045
GM-CSF	2.966	2.194	0.043

Figure 18. Cytokine profile of alpha SMA positive alpha 10 beta 1 expressing fibroblasts. Human fibroblasts (FB) were resuspended in serum free medium and allowed to incubate for 24 hours. Twenty-four hour serum free conditioned medium (CM) was collected and concentrated 10X. Concentrated fibroblast CM was analyzed for cytokine expression using a Multi-Analyte array ELISA.

Expression of Cytokines from alpha 10 beta 1 expressing fibroblasts attached to distinct ECM substrates. As outlined in specific aim 2, we sought to explore the possible role of alpha 10 beta 1 integrin-mediated binding to distinct forms of collagen might have on cytokine expression from fibroblasts. To this end, alpha 10 beta 1 expressing fibroblasts were seeded on either intact native collagen or denatured collagen under serum free conditions. Twenty-four hours later conditioned medium was collected and examined for differential expression of cytokines using a Multi-Analyte ELISA assay kit. As shown in figure 19, while the majority of cytokines examined showed little change between the distinct culturing conditions, however, a reduction by nearly 2-fold in the levels of INF-gamma was observed in CM from fibroblasts cultured on denatured collagen as compared to intact native collagen.

Cytokine	Native Coll-1	Denatured Coll-I
IL-1α	0.398	0.385
IL-1β	0.436	0.436
IL-2	0.514	0.490
IL-4	0.430	0.468
IL-6	2.430	2.701
IL-8	3.621	3.606
IL-10	0.423	0.445
IL-12	0.544	0.436
IL-17A	1.729	1.862
INFγ	0.741	0.487
TNF-α	0.436	0.389
GM-CSF	0.991	0.719

Figure 19. Expression of Cytokines from alpha 10 beta 1 expressing fibroblasts attached to distinct ECM substrates. Human fibroblasts were resuspended in serum free medium and allowed to attach to either intact collagen coated wells or wells coated with denatured collagen for 24 hours. Twenty-four hour serum free conditioned medium (CM) was collected and concentrated 10X. Concentrated fibroblast CM was analyzed for cytokine expression using a Multi-Analyte array ELISA.

Characterization of alpha 10-integrin expression in transgenic alpha 10 beta 1 knockout mouse model. As outlined in specific aim 1, we sought to examine the role of alpha 10 beta 1 integrin in regulating ovarian tumor growth in vivo. In this regard, we established a transgenic alpha 10 beta 1 integrin-knockout mice in our laboratory. To confirm the status of the expression of alpha 10 integrin in these mice genotyping was carried out on wild type, heterozygous and homozygous transgenic mice for alpha 10 integrin (covering intron 6/7 and exon 8). As shown in figure 20A, while wild type and heterozygous mice expressed alpha 10 integrin, we failed to detect alpha 10 beta 1 in the homozygous mice. Moreover, the transgenic targeting construct, which included a LacZ gene and En2 cassette, which were readily detected in the homozygous mice. In addition, RT-PCR was carried out using isolated cartilage cells, a known source of alpha 10 integrin. As shown in figure 20B, alpha 10 integrin was readily detected in cells from wild type mice while we failed to detect alpha 10 integrin in cartilage cells from homozygous knock out mice. These data confirm the utility of these transgenic mice as an alpha 10 beta 1 integrin knockout model for our studies.

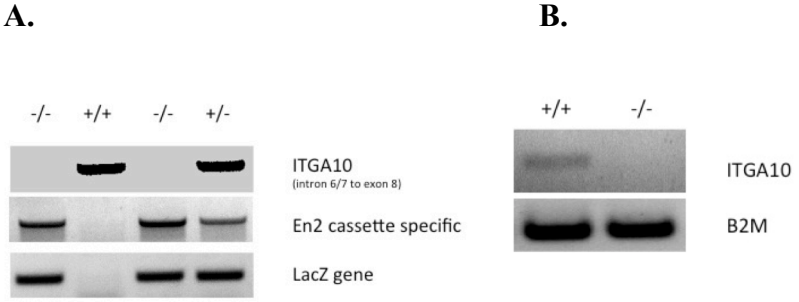

Figure 20. Characterization of alpha 10 integrin expression in transgenic alpha 10 beta 1 knockout mouse model. A). Genotyping analysis of wild type (+\+) heterozygous (+\-) and homozygous (-/-) transgenic alpha 10 knock out mice for expression of alpha 10 integrin, and the En2 cassette and Lac Z gene within the targeting construct. B). Expression (RT-PCR) of alpha 10-integrin gene in cartilage cells isolated from wild type (+/+) and homozygous alpha 10 knock out mice (-/-).

Characterization of ID8 ovarian tumors growing in wild type and alpha 10 integrin knockdown mice. As outlined in specific aim 1, we sought to examine the growth and characterize ID8 ovarian tumors in mice in which integrin alpha 10 beta 1 knocked down. To begin these studies, we first injected ID8 cell i.p into either wild type or homozygous transgenic alpha 10 knock down mice. As shown in figure 21, i.p injection of ID8 tumor cells in wild type mice resulted in scattered small i.p tumors throughout the peritoneal cavity of the

mice. Giemsa stain of these tumors growing in wild type mice indicated extensive stromal cell infiltration with multiple blood vessels (arrows). Interestingly, fewer ID8 tumor lesions were detected in alpha 10-integrin knock down mice and while specific quantification will be needed, our preliminary analysis suggested that these ID8 tumors tended to be smaller in size. Moreover, these ID8 tumors also tended to have less stromal cell infiltration and fewer blood vessels. Further analysis and quantification will be needed to confirm these important preliminary observations.

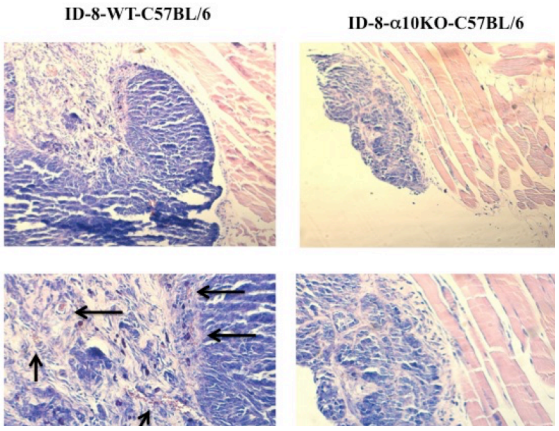

Figure 21. Characterization of ID8 ovarian tumors growing in wild type and alpha 10 integrin knockdown mice. Wild type (+\+) left or homozygous (-/-) transgenic alpha 10 knock out mice right were injected (i.p) with $5x10^6$ ID8 ovarian tumor cells. Tumors were allowed to grow for 6 weeks. Mice were sacrificed and i.p tumors were examined. Frozen sections of small i.p tumors (N=4) from each condition were stained by Giemsa for analysis. Top), representative examples of ID8 tumors (100x). Bottom), representative examples of ID8 tumors (200x). Arrows indicate tumor associated blood vessels.

Reduced growth of ID8 ovarian tumors in alpha 10 integrin knockdown mice. As outlined in specific aim 1, we sought to examine the growth and characterize ID8 ovarian tumors in mice in which the integrin alpha 10 beta 1 was knocked down. ID8 tumor cells were injected in either wild type or alpha 10 knock down mice. The growth of murine ID8 ovarian tumors in alpha 10 beta 1 knock out mice was significantly ($P<0.05$) reduced as compared to tumor growth in wild type mice (Fig 22A). These studies suggest that alpha 10 beta 1 expressed in host stromal cells may play a significant role in regulating ovarian tumors growth in vivo. Importantly, the majority of alpha 10 beta 1 is expressed within the stromal CAF-like infiltrates of ovarian tumors rather than the tumor cells. Given these findings, and published studies indicating an important role for CAF-like stromal cells in controlling immune cell function and T-cell infiltration, we sought to examine the levels of CD8+ T-cells within tumors growing in each mouse variant. In a preliminary study, reduced levels alpha SMA (Red) expressing stromal cells were detected in ID8 tumors growing in alpha 10 beta 1 K/O mice as compared to control (fig 22B) and interestingly, elevated levels of CD8+ T-cells (Green) were detected in alpha 10-K/O mice (figs 22B and C). While quantification will be required to confirm these observations, these results are consistent with the possibility that alpha SMA-expressing CAF-like cells contribute to immune suppression and possibly the lower level of CD8+ T-cell in wild type mice. Conversely, the reduced levels of alpha SMA-expressing cells in ID8 tumors growing in alpha 10-K/O mice may allow enhanced levels of cytotoxic CD8+ T-cells to enter the these tumors resulting in reduced tumor growth.

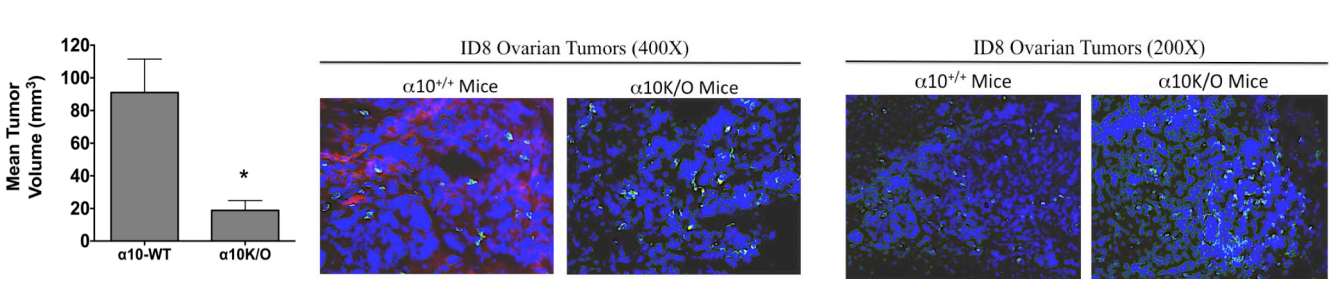

Figure 22. Reduced growth of murine ID8 ovarian tumors in alpha 10 beta 1 knock out mice. Murine ID8 tumor cells were injected in either alpha 10 beta 1 wild type mice (alpha 10-WT) or alpha 10 beta 1knockout (alpha 10K/O) mice. A). Quantification of tumor size. Data bars represent mean tumor volume ± SEM. N=5-6 per condition. B). Co-expression of alpha SMA positive CAF-like cells (red) and CD8+ T-cells (Green). C). Examples of expression of CD8+ T-cells (green).

Opportunities for training and professional development: Nothing to report

How were the results disseminated to communities of interest: Nothing to report.

Plans for next reporting period: Nothing to report (final report).

4) Impact:

A) What was the impact on the development of the principal discipline of the project? Completion of the project resulted in new cellular and molecular insight into the role of the little understood integrin alpha 10 beta 1 expressed in fibroblasts to regulate ovarian tumor growth. The experimental results of the study are detailed in the final report and in the attached (appendix) published paper. Specifically, our novel studies have defined for the first time, that structural remodeling of the collagenous extracellular matrix within ovarian tumors can result in the selective generation of a novel cryptic collagen epitope that we have termed HU177. Importantly we have shown that this cryptic ECM epitope can bind directly to the collagen binding integrin alpha 10 beta 1, which was shown to be expressed in a subset of alpha SMA expressing cancer associate fibroblasts (CAFs) and help regulate cellular migration. Moreover, our studies also provide exciting new evidence that selective targeting of this cryptic collagen epitope may provide a clinically relevant new strategy to control malignant ovarian tumor. Finally, extension of these studies has resulted in the surprising new observations that integrin alpha 10 beta 1 may also be expressed in T-cells. Given these new findings and the fact that CAF-like cells have been shown to help create an immunosuppressive microenvironment, coupled with our new observations that SKOV-3 tumors growing in alpha10 null mice are smaller and appear to have elevated levels of CD8+ T-cells as compared to wild type mice, are consistent with the possibility that alpha 10 beta 1 integrin signaling may play a role in regulating immune suppression. Given the important role of immune suppressive mechanisms regulating ovarian tumor growth, our new studies may open up new insight into the development of more effective new combination treatment strategies for malignant ovarian tumors.

B) What was the impact on other disciplines? Given that CAFs are thought to play a functional role in multiple types of tumors outside of ovarian cancer, our new studies provide important molecular insight into the roles of alpha 10 beta 1 integrin expression in tumor-associated stromal cells in a variety of tumor types. In addition, our novel observations suggesting that alpha 10 beta 1 may be expressed in T-cells and play a functional role in regulating accumulation of CD8+ T-cell. Interestingly, the immune checkpoint molecule PD-L1 was highly expressed in alpha 10 beta 1 expressing CAF-like cells that were localized in close proximity to the HU177 collagen epitope. Thus, our novel studies may provide new insight into the mechanism that control immune suppression.

C) What was the impact on technology transfer? Nothing to report

D) What was the impact on society beyond science and technology? Nothing to report**.**

5) Changes/Problems: nothing to report

6) Products:

A) Publication: A manuscript reporting many of the experimental findings was published in the American Journal of Pathology. (Caron, J. M., Ames, J. J., Contois, L., Liebes, L., Friesel, R. E., Vary, C. P. H., Oxburg, L., and Brooks, P. C. Inhibition of ovarian tumor growth by targeting the HU177 cryptic collagen epitope. AM. J. Pathol: 2016; 186: 1649-1661). A copy of the published paper is provided in the appendix.
The DoD grant was acknowledged.

B) Websites: nothing to report:

C) Technologies and techniques: nothing to report

D) Inventions, Patent applications, and/or licenses: A US patent application was filed in June of 2016. Title: Enhancing the therapeutic activity of immune checkpoint inhibitors. US application number: 62169463

7) Participants and Other Collaborating Organizations

A) What individuals have worked on the project?

Name	**Peter Brooks**
Project Role	**Principal Investigator**
Nearest Person Month Worked	**2.5 calendar months**
Contribution to Project	**Provides overall scientific direction, analysis, writes manuscripts, supervises lab technician**
Funding Support	

Name	**Jennifer Caron**
Project Role	**Laboratory Technician**
Nearest Person Month Worked	**4.4 calendar months**
Contribution to Project	**Conducted biochemical and animal experiments**
Funding Support	

B) Has there been a change in Active Other Support for PD/PI or senior/key since last reporting period? Yes.

Maine Cancer Foundation grant ended December 31, 2015.

C) What other organizations were involved as partners? Nothing to report.

8) Special Reporting Requirements. None.

9) APPENDICES:
Publications: Caron, J. M., Ames, J. J., Contois, L., Liebes, L., Friesel, R. E., Vary, C. P. H., Oxburg, L., and Brooks, P. C. Inhibition of ovarian tumor growth by targeting the HU177 cryptic collagen epitope. AM. J. Pathol: 2016; 186: 1649-1661. PMCID: PMC4901133 (available 6/1/2017). (see attached).

The American Journal of Pathology, Vol. 186, No. 6, June 2016

The American Journal of
PATHOLOGY
ajp.amjpathol.org

TUMORIGENESIS AND NEOPLASTIC PROGRESSION

Inhibition of Ovarian Tumor Growth by Targeting the HU177 Cryptic Collagen Epitope

Jennifer M. Caron,* Jacquelyn J. Ames,* Liangru Contois,* Leonard Liebes,* Robert Friesel,* Franco Muggia,† Calvin P.H. Vary,* Leif Oxburgh,* and Peter C. Brooks*

From the Maine Medical Center Research Institute, Center for Molecular Medicine, Scarborough, Maine; and the New York University Langone Medical Center,† Division of Hematology and Medical Oncology, New York, New York*

Accepted for publication January 19, 2016.

Address correspondence to Peter C. Brooks, Ph.D., Maine Medical Center Research Institute, Center for Molecular Medicine, 81 Research Dr., Scarborough, ME 04074. E-mail: brookp1@mmc.org.

Evidence suggests that stromal cells play critical roles in tumor growth. Uncovering new mechanisms that control stromal cell behavior and their accumulation within tumors may lead to development of more effective treatments. We provide evidence that the HU177 cryptic collagen epitope is selectively generated within human ovarian carcinomas and this collagen epitope plays a role in SKOV-3 ovarian tumor growth *in vivo*. The ability of the HU177 epitope to regulate SKOV-3 tumor growth depends in part on its ability to modulate stromal cell behavior because targeting this epitope inhibited angiogenesis and, surprisingly, the accumulation of α-smooth muscle actin—expressing stromal cells. Integrin α10β1 can serve as a receptor for the HU177 epitope in α-smooth muscle actin—expressing stromal cells and subsequently regulates Erk-dependent migration. These findings are consistent with a mechanism by which the generation of the HU177 collagen epitope provides a previously unrecognized $\alpha_{10}\beta_1$ ligand that selectively governs angiogenesis and the accumulation of stromal cells, which in turn secrete protumorigenic factors that contribute to ovarian tumor growth. Our findings provide a new mechanistic understanding into the roles by which the HU177 epitope regulates ovarian tumor growth and provide new insight into the clinical results from a phase 1 human clinical study of the monoclonal antibody D93/TRC093 in patients with advanced malignant tumors. *(Am J Pathol 2016, 186: 1649—1661; http://dx.doi.org/10.1016/j.ajpath.2016.01.015)*

The importance of stromal cells, such as endothelial cells, fibroblasts, pericytes, and inflammatory infiltrates, in tumor growth has been appreciated for years.[1—4] This insight has led investigators to begin developing novel approaches to regulate stromal cell behavior.[5—8] However, given the functions of stromal cells in normal physiologic processes, it is important to create strategies that might restrict the effect on stromal cells to that within the tumor microenvironment. In this regard, the structures of extracellular matrix (ECM) proteins that compose the architectural framework of most normal tissues are largely intact. In contrast, tumors often exhibit an altered ECM structure with proteolytically degraded matrix proteins.[9,10] This differential ECM configuration might provide a unique means of selectively regulating stromal cell behavior within tumors because cellular interactions with remodeled or denatured matrix proteins, such as collagen, alters adhesion, migration, proliferation, and survival.[11—14]

Our previous studies uncovered functional cryptic sites within ECM molecules.[14—16] We have likened the process of generating cryptic elements to that of a biomechanical ECM switch in which structural alterations in these molecules initiated by either proteolytic cleavage or other physical mechanisms lead to the generation of cryptic regulatory epitopes, which contribute to the initiation of unique signaling cascades that facilitate angiogenesis, tumor growth, and metastasis.[11—17] Recently, we identified a new cryptic ECM epitope present within multiple forms of collagen.[15] The HU177 epitope was generated within the ECM of angiogenic vessels and regulates endothelial cell

Supported by NIH grant CA91645 and Department of Defense grant from the Ovarian Cancer Research Program award W81XWH-13-OCRP-PA (P.C.B.). Additional support was from NIH grants HL65301 (R.F.) and HL083151, American Heart Association grant GRNT20460045 (C.P.H.V.), a Chemotherapy Foundation grant (L.L.), Bioinformatics Core grant P20 RR181789 (D.M.W.), NIH grants 5P30GM103392 (R.F.) and ROIDK078161 (L.O.), and institutional support from the Maine Medical Center.

Disclosures: P.C.B., C.P.H.V., and L.L. hold an equity position in CryptoMedix, LLC.

http://dx.doi.org/10.1016/j.ajpath.2016.01.015

behavior because a monoclonal antibody (mAb) directed to this epitope selectively inhibited endothelial cell adhesion and migration on denatured collagen and blocked angiogenesis *in vivo*.[15] This antibody was humanized (mAb D93/TRC093) and a phase 1 human clinical trial was completed.[18–20] Clinical findings suggested that the HU177 epitope plays a role in tumor growth because 26% of the treated patients exhibited stable disease and a reduction in liver lesions was observed in a patient with ovarian cancer.[20]

Ovarian cancer is a heterogeneous disease classified by distinct histologic subtypes.[21–25] The molecular complexity of these tumors is indicated by the fact that low-grade type 1 tumors often exhibit alterations in KRAS, BRAF, and PTEN, whereas high-grade type 2 tumors often have alterations in TP53 and BRCA1/2.[21–25] Importantly, stromal cells, such as endothelial cells and activated fibroblasts, may contribute to the development of ovarian carcinoma.[26–28] Although collagen remodeling occurs during ovarian tumor growth, it is not known whether these changes are sufficient to generate the HU177 epitope or what role it plays in ovarian tumor growth.

We present evidence that the HU177 cryptic collagen epitope is abundantly generated within human ovarian tumors, whereas little is expressed in benign granulomas. Antibodies directed to this epitope inhibited SKOV-3 tumor growth *in vivo*, which was accompanied by reductions in proliferation, angiogenesis, and the accumulation of α-smooth muscle actin (α-SMA)–expressing stromal cells. Although our studies indicate that the $\alpha_2\beta_1$ integrin can bind the HU177 site, the little understood integrin $\alpha_{10}\beta_1$ plays an important role as a functional receptor in α-SMA–expressing stromal cells. Blocking interactions of the HU177 collagen epitope with $\alpha_{10}\beta_1$ integrin–expressing fibroblasts reduced fibroblast growth factor (FGF)-2–stimulated Erk phosphorylation and migration on denatured collagen. Given the emerging roles of fibroblast-like cells in promoting tumor growth, these findings are consistent with a mechanism by which blocking the HU177 epitope reduces $\alpha_{10}\beta_1$-dependent accumulation of α-SMA–expressing stromal cells in ovarian tumors, leading to the reduction of an important source of protumorigenic cytokines that contribute to tumor progression.

Materials and Methods

Reagents, Chemicals, and Antibodies

Collagen type I was from Sigma (St Louis, MO). Denatured collagen was prepared by boiling the solution of commercially obtained collagen for 15 minutes. The denatured collagen was allowed to cool for 5 minutes before use. FGF-2; integrins $\alpha_1\beta_1$, $\alpha_2\beta_1$, $\alpha_3\beta_1$, $\alpha_{10}\beta_1$, and $\alpha_v\beta_3$; and antibodies directed to α_1, α_2, α_v integrins, and IL-6 were from R&D Systems (Minneapolis, MN). Anti-CD31 antibody was from BD Pharmingen (San Diego, CA). Anti–α-SMA and anti–Ki-67 antibodies were from Abcam (Cambridge, MA). Anti-Erk antibodies were from Cell Signaling Technology (Danvers, MA). Anti–collagen 1 antibody was from Rockland (Gilbertsville, PA). Antibody to $\alpha_{10}\beta_1$ was from Novus Biologicals (Littleton, CO). BrdU kit was from Millipore (Bedford, MA). Secondary antibodies were from Promega (Madison, WI). mAb HU177 was developed in our laboratory and found to bind a PGxPG-containing epitopes exposed within denatured but not intact collagen from multiple species.[11–16] mAb D93/TRC093 is a humanized version of mAb HU177 that also binds the PGxPG-containing epitopes within denatured collagen from multiple species and was obtained from TRACON (San Diego, CA). The control antibody (mAb XL166) was generated in our laboratory and is directed to an RGD collagen epitope. Synthetic collagen peptide PGF (CPGFPGFC) and control peptides (CQGPSGAPGEC, CTWPRHHTTDALL, and CNSYSYPSLRSP) were from QED Biosciences (San Diego, CA). MEK inhibitor (PD98059) was from CalBiochem (San Diego, CA).

Analysis of Tissue Antigens

Human ovarian tissues were from Maine Medical Center under institutional review board exempt protocol. For quantification of the HU177 epitope, biopsy specimens ($n = 9$) from high-grade ovarian tumors (serous and endometrial) or benign ovarian granulomas ($n = 9$) were stained with mAb HU177. Ornithine carbamoyltransferase compound–embedded frozen sections (4.0 μm) of biopsy specimens of human ovarian tumor tissues were stained by routine hematoxylin and eosin procedure or immunofluorescence. Immunofluorescence staining was performed on frozen sections by first blocking the tissue sections with 1.0% bovine serum albumin (BSA) in phosphate-buffered saline (PBS) for 1 hour followed by washing three times with PBS. Tissue sections were next incubated with 100 μg/mL of anti-HU177 antibody for 1 hour at room temperature. Tissues sections were next washed three times with PBS followed by incubation with fluorescein isothiocyanate–labeled secondary antibody for 1 hour. For quantification, stained tissue sections were scanned using Kodak ID system and pixel density quantified from five 200× fields from each of the five specimens from each condition using Molecular Analyst Software version 2.1 (Kodak, Stamford, CT).[29] Tumors were analyzed for apoptosis using terminal deoxynucleotidyl transferase-mediated dUTP nick-end labeling staining, for proliferation using anti–Ki-67 antibody staining (1:1000), for angiogenesis using anti-CD31 antibody staining (1:300), and for carcinoma-associated fibroblast (CAF)–like stromal cells using a combination of anti–α-SMA (1:1000), anti–platelet-derived growth factor receptor α (1:500), and anti–fibroblast activation protein (1:300) antibody staining. Quantification was performed within five 200× fields from each of three to five tumors.

Cells and Cell Culture

SKOV-3 cells were from ATCC (Manassas, VA) and cultured in RPMI 1640 medium in the presence of 5% fetal bovine serum. Human umbilical vein endothelial cells were obtained from Lonza (Walkersville, MD) and cultured in endothelial basal medium 2 in 2% fetal bovine serum and supplements (Lonza). Human dermal fibroblasts were obtained from Science Cell (Carlsbad, CA) and cultured in medium with 2.0% fetal bovine serum.

Solid-Phase Binding Assays

Plates were coated with 25 μg/mL of native or denatured (boiled for 15 minutes) collagen. Collagen epitope peptide PGF and control peptides were immobilized at 100 μg/mL. Integrins (0 to 2.0 μg/mL) were diluted in binding buffer that contained 20 mmol/L Tris, 15 mmol/L NaCl, 1 mmol/L $MgCl_2$, 0.2 mmol/L $MnCl_2$, and 0.5% BSA (pH 7.4) as described.[13] Integrins were allowed to bind for 1 hour and plates washed and incubated with anti-integrin antibodies (1:100 dilution) for 1 hour. Plates were washed and incubated with horseradish peroxidase–labeled secondary antibodies (1:5000 dilution). In a second assay, 0.5-μg/mL integrins were coated in binding buffer, plates were washed and blocked as before, and 0 to 10.0 μg/mL of denatured (boiled for 15 minutes) collagen was added. Denatured collagen was detected with anticollagen antibody (1:1000). For integrin-blocking enzyme-linked immunosorbent assay, wells were coated with denatured collagen and pretreated with 0.1 μg/mL of anti-HU177 or control antibody. After washing, wells were incubated with 2.0-μg/mL integrins, and binding was detected as described. Assays were performed at least three times.

Cell Adhesion Assays

The wells of nontissue culture 48-well cluster plates were coated for 12 hours at 4°C with 5 μg/mL of native or denatured (boiled for 15 minutes) collagen prepared as described above. SKOV-3 and fibroblasts were suspended in adhesion buffer that contained RPMI 1640 medium, 1 mmol/L $MgCl_2$, 0.2 mmol/L $MnCl_2$, and 0.5% BSA,[13] and 1×10^5 cells were added in the presence or absence of 100 μg/mL of anti-HU177 or control antibodies. Cells were allowed to attach for 25 minutes. Nonattached cells were removed by washing and attached cells stained with crystal violet as described.[13] Wells were washed and the cell-associated crystal violet was eluted with 100 μL per well of 10% acetic acid. Cell adhesion was quantified by measuring the optical density of the eluted crystal violet as described.[15] Assays were completed at least three times.

Cell Migration Assays

Transwell membranes (8.0-μm pore size) were coated with 5 μg/mL of native or denatured collagen for 12 hours at 4°C as described previously.[13] Migration buffer that contained RPMI 1640 medium, 1 mmol/L $MgCl_2$, 0.2 mmol/L $MnCl_2$, and 0.5% BSA in the presence or absence of 5× concentrated serum free SKOV-3 conditioned medium (CM) or 20 ng/mL of FGF-2 was placed in the lower chambers. SKOV-3 or fibroblasts (1×10^5) were resuspended in migration buffer that contained RPMI 1640 medium, 1 mmol/L $MgCl_2$, 0.2 mmol/L $MnCl_2$, and 0.5% BSA in the presence or absence of 10 μg/mL of antibodies directed to the HU177 epitope, $\alpha_{10}\beta_1$, or 100 μmol/L of the MEK inhibitor (PD98054). Cells were added to the top chamber and allowed to migrate from 2 to 4 hours. Cells that remained on the top of the membranes were removed, and cells that had migrated to the underside of the membrane were quantified by direct cell counts of crystal violet–stained cells or by measuring the optical density of eluted cell-associated crystal violet dye as previously described.[15] Assays were completed at least three times.

Cell Proliferation Assays

To prepare serum free fibroblast CM, 2.0×10^6 cells were seeded in the presence of serum for 2 hours. Serum-containing medium was removed, cells were washed, and serum free RPMI 1640 medium was added. Serum free medium was collected at 24 hours and concentrated 10-fold. SKOV-3 cells were resuspended in the presence (150 μL) of control (10×) RPMI 1640 medium or (10×) fibroblast CM. Cells were added to wells and allowed to growth for 24 or 72 hours. Cell proliferation was quantified at 24 or 72 hours using BrdU kit according to manufacturer's instructions. Assays were completed three times.

Tumor Growth Assays

Briefly, chorioallantoic membranes (CAMs) of 10-day-old chicks ($n = 6$ to 8) were prepared as described[13] by separating the CAM from the shell membrane. Single-cell suspensions of SKOV-3 cells (3×10^6) were applied topically to the CAMs in a total volume of 40 μL.[30] Twenty-four hours later embryos were either untreated or treated with a single topical application of 100 μg of anti-HU177 antibody or control nonspecific antibody (100 μg per embryo) in a total volume of 40 μL. Tumors were allowed to grow for a total of 7 days. At the end of the 7-day growth period, the embryos were sacrificed, the tumors dissected, and wet weights determined as described previously.[13] For murine experiments, nude (NCRNU-F) mice ($n = 6$ to 8) were injected subcutaneously into the flanks with 3.0×10^6 SKOV-3 cells per mouse. Mice were allowed to form tumors for 5 days and then untreated or injected (i.p.) with 0 to 100 μg/mL of mAb D93 or control antibody three times per week for 28 days. Tumors were measured with calipers and volumes calculated as $V = L^2 \times W/2$, where V indicates volume; L, length; and W, width. Experiments were completed three times.

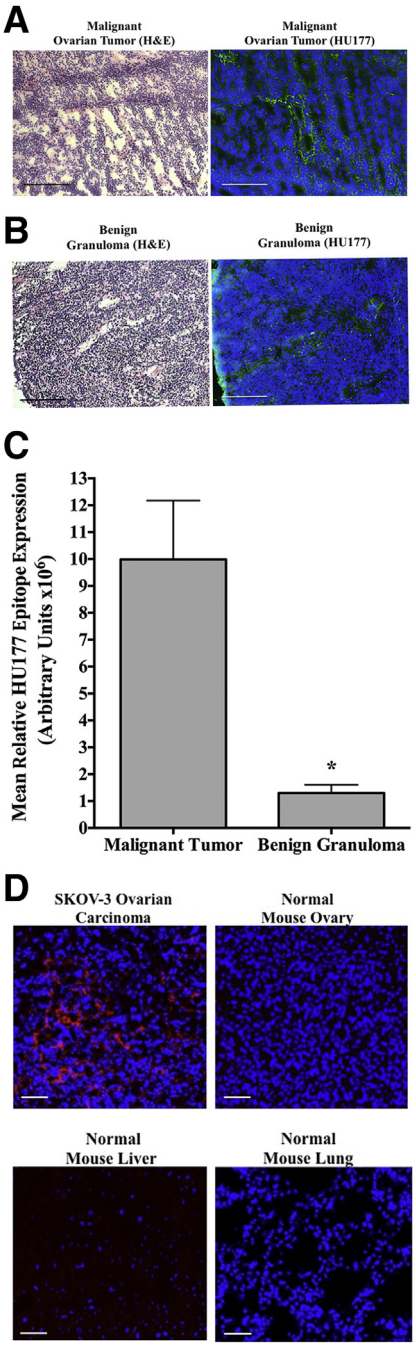

Figure 1 Generation of the HU177 epitope in ovarian tumors. Biopsy specimens from frozen sections of malignant human ovarian tumors or benign granulomas were stained with hematoxylin and eosin (H&E) or with anti-HU177 antibody. Examples of H&E staining or staining for the HU177 cryptic collagen epitope in malignant ovarian tumors (**A**) or benign granulomas (**B**). **C:** Quantification of the relative levels of HU177 epitope within malignant ovarian tumors or benign granulomas. **D:** Examples of HU177 epitope (red) within SKOV-3 tumors or normal ovaries, lungs, and liver. Data are expressed as means ± SEM from five fields (**C**). *$P < 0.05$ compared with controls. Scale bars = 63 μm. Original magnification, ×200.

Western Blot Analysis

Cells from culture or cells seeded on native or denatured (boiled for 15 minutes) collagen type I–coated plates were allowed to attach for 15 minutes, then they were lyzed in radioimmunoprecipitation assay buffer (Santa Cruz, CA) with 1× protease inhibitor cocktail. Lysates were separated by SDS-PAGE and probed with antibodies directed to α_{10}, α_1 integrins, total and phosphorylated Erk, Ki-67, β-tubulin, or actin. Assays were performed at least three times.

Cytokine Analysis of Fibroblast CM

A total of 50 μL of serum free CM was screened for a panel of 12 cytokines (IL-1α, IL-1β, IL-2, IL-4, IL-6, IL-8, IL-10, IL-12, IL-17A, tumor necrosis factor-α, interferon-γ, and granulocyte-macrophage colony-stimulating factor) using the Multi-analyte ELISArray kit (Qiagen, Valencia, CA) according to the manufacturer's instructions. Analysis of conditioned medium was completed twice.

Statistical Analysis

Statistical analysis was performed using Graph Pad Instat for Mac version 3.0b (Graphpad Software Inc, La Jolla, CA). Data were analyzed for significance using the *t*-test. $P < 0.05$ was considered significant.

Results

Differential Generation of the HU177 Epitope in Ovarian Tumors

Studies have correlated enhanced collagen synthesis and ECM degradation with tumor progression.[31,32] In this regard, we examined biopsy specimens of human ovarian tumors and benign granulomas for expression of the HU177 cryptic collagen epitope. Serial sections from frozen tissues were stained by hematoxylin and eosin or with anti-HU177 antibody. The HU177 cryptic collagen epitope (green) could be detected in the ECM of malignant ovarian tumors (Figure 1A), whereas minimal detection was observed in the ECM of the benign ovarian lesions (Figure 1B). Quantification of the relative levels of the HU177 cryptic collagen epitope (Figure 1C) indicated a significant ($P < 0.05$) increase in HU177 collagen epitope in tumors compared with the benign lesions. To confirm the generation of the HU177 epitope in an experimental mouse model, we examined its expression of the HU177 collagen epitope in SKOV-3 tumors growing in mice. Although HU177 epitope was detected within the SKOV-3 tumors, little was observed in normal tissues, including ovaries, liver, and lungs (Figure 1D). These findings are consistent with the restricted generation of the collagen epitope.

The HU177 Epitope Regulates Ovarian Tumor Growth

Given the differential generation of the HU177 epitope observed *in vivo*, we determined whether the HU177 epitope plays a functional role in ovarian tumor growth. To examine this possibility, SKOV-3 ovarian tumor cells were seeded topically

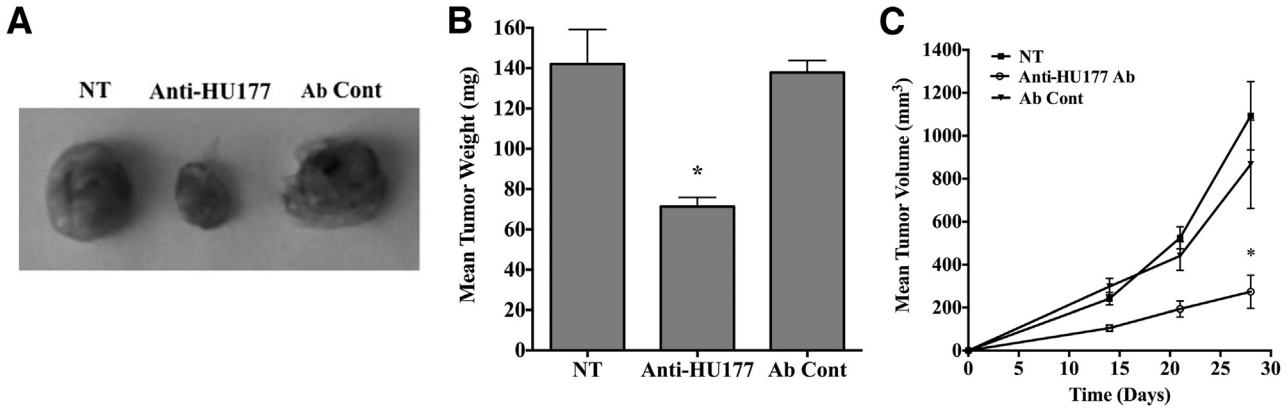

Figure 2 Inhibition of tumor growth by targeting the HU177 epitope. **A** and **B:** SKOV-3 cells were seeded topically on the chorioallantoic membranes of chick embryos. Twenty-four hours later, the animals were not treated (NT) or treated once topically with 100 μg of anti-HU177 or 100 μg of control antibody (Ab Cont). **A:** Examples of tumors from each condition. **B:** Quantification of mean tumor weights from each condition after a 7-day incubation period. **C:** Mice were injected s.c. in the flanks with SKOV-3 cells and 5 days later were untreated or treated i.p. with 100 μg of anti-HU177 antibody or Ab Cont three times per week for 28 days. Data are expressed as means ± SEM of tumor weights (**B**) and tumor volume (**C**). $n = 7$ to 8 animals per condition (**B**); $n = 5$ to 6 animals per condition (**C**). *$P < 0.05$ compared with controls.

on the CAM of chick embryos. Twenty-four hours later the embryos were either not treated or treated with a single topical application with anti-HU177 antibody or nonspecific control. After 7 days of incubation, the resulting tumors were dissected from the CAMs for analysis. SKOV-3 tumors dissected from chick embryos treated with anti-HU177 antibody were smaller than controls (Figure 2A). Quantification indicated that targeting the HU177 epitope significantly ($P < 0.05$) inhibited SKOV-3 tumor growth by approximately 50% compared with controls (Figure 2B). To confirm these findings in a murine model, SKOV-3 cells were injected subcutaneously into the flanks of nude mice. Five days after establishment of small tumor lesions, mice were either untreated or treated (100 μg per mouse three times per week) i.p. with anti-HU177 mAb or control nonspecific antibody. Treatment with anti-HU177 antibody significantly ($P < 0.05$) reduced tumor size by approximately 70% by day 28 (Figure 2C). Dose-dependent studies indicated inhibition of tumor growth at doses of anti-HU177 antibody as low as 10 μg per mouse three times per week (data not shown).

The HU177 Epitope Regulates Angiogenesis and Stromal Cell Accumulation in Ovarian Tumors

The behavior of multiple cell types within the tumor microenvironment, including stromal cells, can be controlled by interactions with collagen.[2,6,33–37] Therefore, we examined apoptosis within control and anti-HU177–treated SKOV-3 tumors using terminal deoxynucleotidyl transferase-mediated dUTP nick-end labeling staining. An approximately 1.8-fold increase in apoptosis was detected within anti-HU177–treated tumors compared with control (data not shown); however, because of variation in staining, this increase did not meet statistical significance. Next, we examined cellular proliferation by quantifying Ki-67 antigen expression within these tumors growing *in vivo*. SKOV-3 tumors from anti-HU177 mAb–treated mice exhibited significantly ($P < 0.05$) reduced (25% to 40%) Ki-67 expression compared with no treatment or control antibody, respectively (Figure 3A). Given previous studies indicating that blocking the HU177 epitope selectively inhibited endothelial cell adhesion to denatured collagen type IV but not native intact collagen type IV[15] and inhibited angiogenesis *in vivo*,[15,18] the reduction in cellular proliferation within these tumors could be due to multiple mechanisms, including inhibition of angiogenesis given the known role of angiogenesis in regulating tumor growth.

To examine the distribution of the HU177 epitope in ovarian tumors, SKOV-3 tumors were co-stained with antibodies directed to the HUI77 epitope and CD31, a marker of blood vessels. Although the HU177 epitope was detected in association with some CD31-positive vessels (Figure 3B), it was more extensively associated with α-SMA–expressing fibroblast-like stromal cells (Figure 3B). Given the close proximity of the α-SMA–expressing stromal cells and blood vessels to the HU177 epitope, it is possible that α-SMA–expressing stromal cells and endothelial cells may interact with this cryptic collagen epitope and regulate their behavior. Therefore, we analyzed the effects of anti-HU177 mAb treatment on SKOV-3 tumor angiogenesis and the accumulation of tumor-associated α-SMA–expressing cells. A significant ($P < 0.05$) 35% inhibition of SKOV-3 ovarian tumor angiogenesis was observed, and remarkably (Figure 3C), a 70% reduction in α-SMA–expressing stromal cells was also detected after treatment with anti-HU177 antibody (Figure 3D), consistent with a possible role for cellular interactions with the HU177 epitope in regulating accumulation of these cells within the tumor. Collectively, these findings are consistent with the notion that reduced angiogenesis and α-SMA–expressing stromal cell accumulation may contribute to the anti-tumor activity observed after selective blockade of the HU177 collagen epitope.

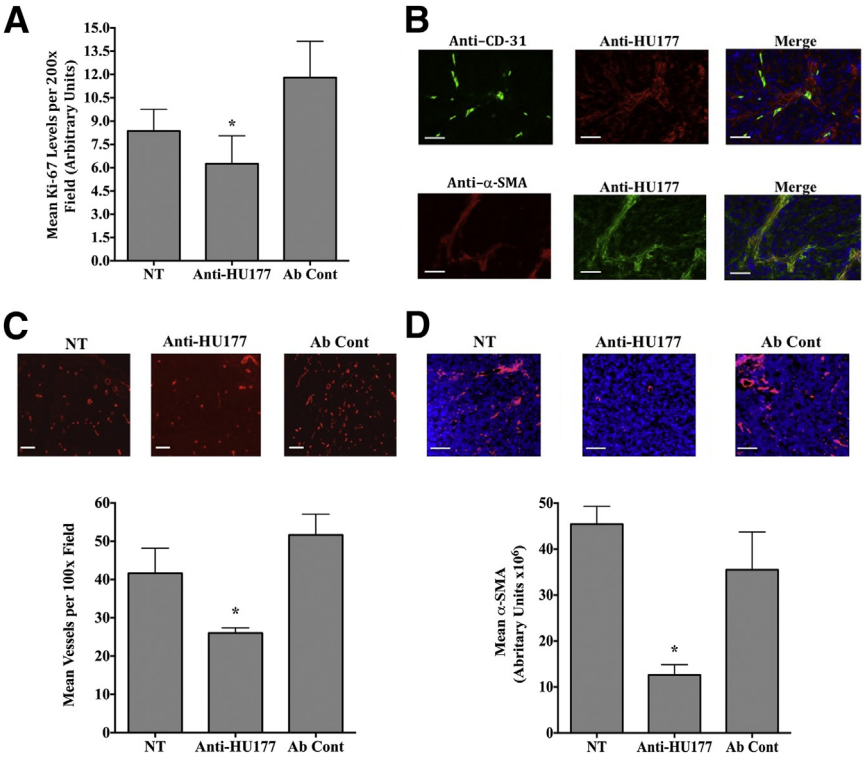

Figure 3 Analysis of SKOV-3 tumors growing in mice. Mice were injected s.c. in the flanks with SKOV-3 cells and after a 5-day incubation period were not treated (NT) or treated i.p. with 100 μg of anti-HU177 or 100 μg of control antibodies (Ab Cont) three times per week for 28 days. **A:** Analysis of the relative levels of Ki-67 expression per 200× field in SKOV-3 tumors. **B:** Example of co-expression of CD31 (green) and HU177 epitope (red) in untreated SKOV-3 tumors and co-expression of α-smooth muscle actin (α-SMA) (red) and HU177 epitope (green) in untreated SKOV-3 tumors. **C:** Mice were injected s.c. in the flanks with SKOV-3 cells and after a 5-day incubation period were either untreated or treated i.p. with 100 μg of anti-HU177 or Ab Cont three times per week for 28 days. Examples of tumors from each condition stained for CD31 (red) and the quantification of tumor angiogenesis per 100× field. **D:** Mice were injected subcutaneously in the flanks with SKOV-3 cells and after a 5-day incubation period were either untreated or treated i.p. with 100 μg of anti-HU177 or Ab Cont three times per week for 28 days. Examples of tumors from each condition stained for α-SMA (red) and the quantification α-SMA–expressing infiltrating stromal cells per 100× field. Data are expressed as means ± SEM (**A**, **C**, and **D**). *$P < 0.05$ compared with controls. Scale bars = 126 μm.

SKOV-3 Tumor Cells and Fibroblast Exhibit Enhanced Adhesion and Migration on Denatured Collagen

Previous studies have documented that changes in the native structure of ECM proteins can alter the ability of cells to bind to these denatured proteins in part by disrupting conformational dependent epitopes required for cell binding in the context of its native configuration and/or exposing previously hidden cryptic binding epitopes, including cryptic arginine-glycine-aspartic acid–containing sequences.[12–16] However, the ability of distinct cell types to interact with denatured collagen may vary widely and likely depends on multiple factors, including the expression and activation of cell surface receptors with the capacity to recognize and bind to the multiple cryptic epitopes exposed after denaturation. To examine whether cellular interactions with denatured collagen alter cellular behavior, we compared SKOV-3 and fibroblast adhesion and migration on native and denatured collagen. A small but significant ($P < 0.05$) enhancement of SKOV-3 (38%) and fibroblast (29%) adhesion was detected on denatured collagen compared with native collagen (Figure 4, A and B). In similar studies, we compared the basal migratory capacity of SKOV-3 and fibroblasts on native and denatured collagen. Again a small but significant ($P < 0.05$) enhancement of SKOV-3 (34%) and fibroblast (19%) migration was detected on denatured collagen compared with native collagen (Figure 4, C and D). Although these studies do not specifically indicate that the enhanced adhesion and migration of the cells on denatured collagen depend specifically on the HU177 epitope, given that multiple cryptic epitopes are exposed after denaturation, these observations, however, indicate that interactions with

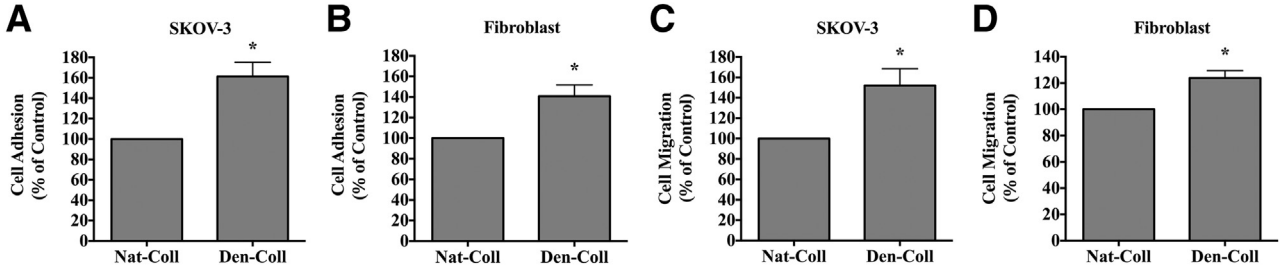

Figure 4 SKOV-3 tumor cells and fibroblast exhibit enhanced adhesion and migration on denatured collagen. Nontissue culture wells and membranes from transwell migration chambers were coated with 5.0 μg/mL of native collagen (Nat-Coll) or denatured collagen (Den-Coll). SKOV-3 cells (**A** and **C**) or fibroblasts (**B** and **D**) were allowed to attach or migrate on either native or denatured collagen. **A:** Quantification of mean SKOV-3 cell adhesion. **B:** Quantification of mean fibroblast cell adhesion. **C:** Quantification of mean SKOV-3 cell migration. **D:** Quantification of mean fibroblast cell migration. Data are expressed as means ± SEM of cell adhesion expressed as a percentage of control with adhesion on native collagen set at 100% (**A**–**D**). $n = 4$ (**A**, **B**, and **D**); $n = 3$ (**C**). *$P < 0.05$ compared with controls.

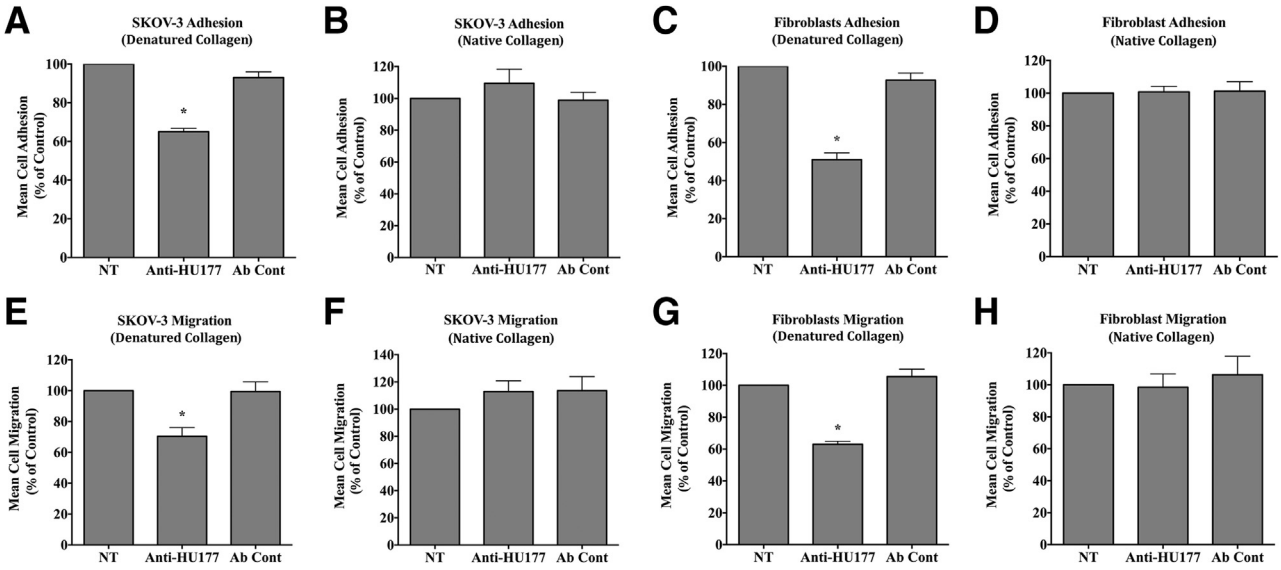

Figure 5 Blocking the HU177 epitope inhibits basal adhesion and migration on denatured collagen. Nontissue culture wells and membranes from transwell migration chambers were coated with 5.0 μg/mL of native collagen or denatured collagen. SKOV-3 cells (**A**, **B**, **E**, and **F**) or fibroblasts (**C**, **D**, **G**, and **H**) were allowed to attach or migrate on either native or denatured collagen in the presence or absence of 50 μg/mL of anti-HU177 antibody or control antibody (Ab Cont). **A** and **B:** Quantification of SKOV-3 cell adhesion to denatured or native collagen in the presence or absence of anti-HU177 or Ab Cont. **C** and **D:** Quantification of fibroblast cell adhesion to denatured or native collagen in the presence or absence of anti-HU177 or Ab Cont. **E** and **F:** Quantification of SKOV-3 cell migration on denatured or native collagen in the presence or absence of anti-HU177 or Ab Cont. **G** and **H:** Quantification of fibroblast cell migration on denatured or native collagen in the presence or absence of anti-HU177 or Ab Cont. Data are expressed as means ± SEM of cell adhesion indicated as a percentage of control with no treatment set at 100% (**A**—**D**) or as means ± SEM of mean cell migration indicated as a percentage of control (**E**—**H**). $n = 4$ to 5 (**A** and **B**); $n = 3$ to 7 (**C** and **D**); $n = 4$ (**E** and **F**); $n = 3$ to 4 (**G** and **H**). *$P < 0.05$ compared with controls. NT, not treated.

denatured collagen can alter the behavior of SKOV-3 cells and fibroblasts *in vitro*.

The HU177 Epitope Regulates SKOV-3 and Fibroblast Adhesion and Migration on Denatured Collagen

Tumor and fibroblast adhesive interactions with denatured collagen, which are present within the microenvironment of malignant cancers, may regulate tumor progression. Given our studies indicating that denaturation of collagen can alter the adhesive and migratory behavior of SKOV-3 cells and fibroblasts, we examined the role of the HU177 collagen epitope on regulating adhesion and migration of these cells. Selectively blocking the HU177 epitope exposed within denatured collagen significantly ($P < 0.05$) inhibited adhesion of SKOV-3 cells to denatured collagen by approximately 40% (Figure 5A). In contrast, the anti-HU177 antibody failed to inhibit adhesion to intact collagen (Figure 5B). These data are consistent with previous studies that report a selective inhibition of cellular interactions with denatured collagen given that the anti-HU177 antibody does not bind native intact collagen.[15–18] In similar studies, we examined the effects of targeting the HU177 epitope on fibroblast adhesion to denatured collagen. Similar to what was observed with SKOV-3 tumor cells, blocking the HU177 epitope significantly ($P < 0.05$) inhibited fibroblast adhesion to denatured collagen by approximately 50% compared with controls, whereas this antibody had no effect on fibroblast adhesion on native intact collagen (Figure 5, C and D). These data indicate that the ability of the anti-HU177 antibody to inhibit adhesion is restricted to those circumstances in which the HU177 epitope is generated; thus, the anti-HU177 antibody does not alter adhesion to intact collagen, thereby allowing a highly selective strategy to inhibit adhesive cellular interactions with denatured collagen.

Next, we examined the migratory capacity of these cells on native and denatured collagen. Blocking the HU177 epitope exposed within denatured collagen also significantly ($P < 0.05$) inhibited basal migration of SKOV-3 and fibroblasts by 35% to 38% (Figure 5, E and F), whereas migration on intact collagen was not effected (Figure 5, E—H). Interestingly, although blocking the HU177 epitope inhibited adhesion and migration, it exhibited little effect on the growth of SKOV-3 cells or fibroblasts on denatured collagen when examined *in vitro* (data not shown). These studies are consistent with the anti-HU177 antibody having minimal if any direct antiproliferative activity on fibroblasts or SKOV-3 cells on denatured collagen *in vitro*.

Inhibition of Growth Factor—Induced Fibroblast Migration by Targeting the HU177 Epitope

Accumulating evidence indicates that recruitment of activated and/or cancer-associated fibroblasts may facilitate tumor growth and survival, in part by providing an important source of protumorigenic factors, including IL-6.[2,5,6,38] Although it is clear that most dermal fibroblast do not represent a fully accurate model of cancer-associated stromal cells

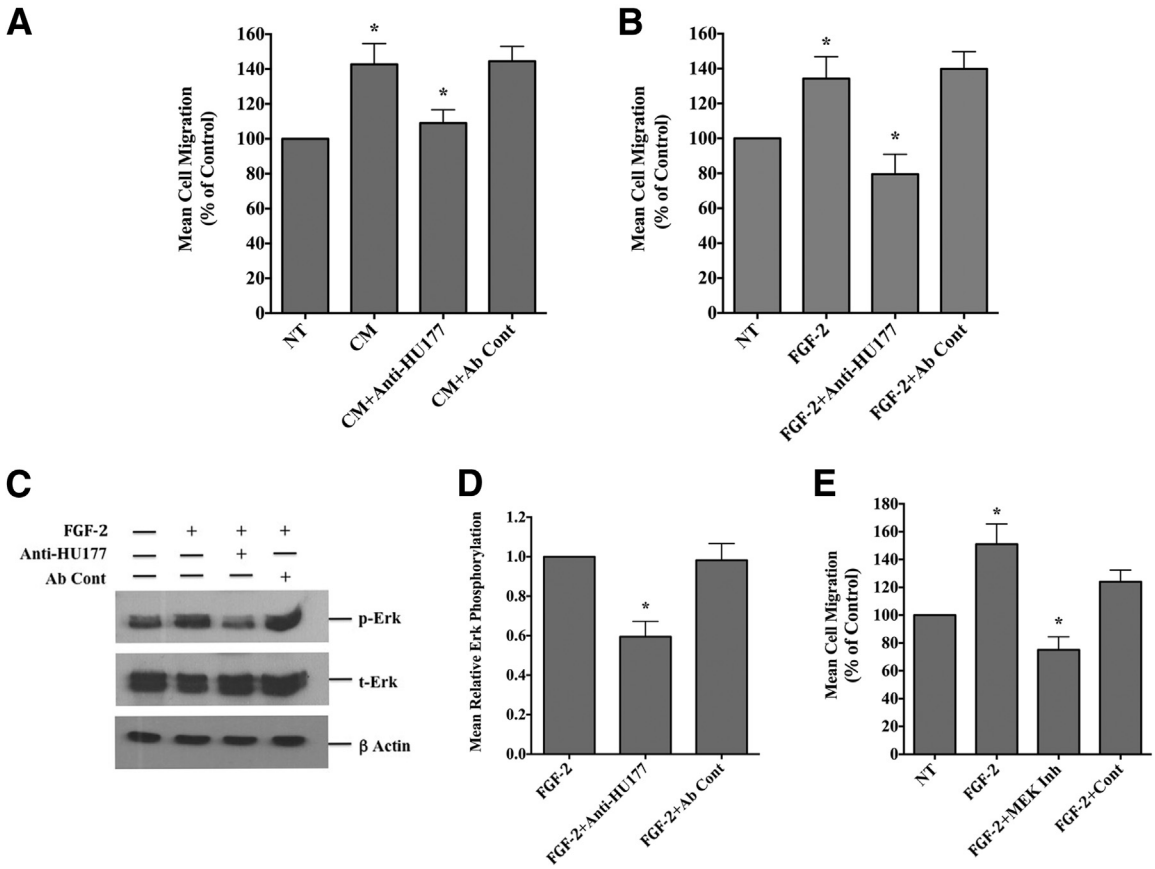

Figure 6 Targeting the HU177 epitope inhibits growth factor–induced migration and Erk phosphorylation. Fibroblasts were resuspended in the presence or absence of SKOV-3 CM (**A**) or fibroblast growth factor (FGF)-2 (**B**) in the presence or absence of 50 μg/mL of anti-HU177 or control antibodies (Ab Cont). **A** and **B:** Quantification of fibroblast cell migration on denatured collagen. **C:** Western blot analysis of Erk in lysates from fibroblasts seeded on denatured collagen in the presence or absence of 50 μg/mL of anti-HU177 or Ab Cont. **D:** Quantification of mean FGF-2–induced Erk phosphorylation in the presence or absence of anti-HU177 antibody or Ab Cont from fibroblasts seeded on denatured collagen. **E:** Fibroblasts were resuspended in the presence or absence of FGF-2 and in the presence or absence of Mek inhibitor and allowed to migrate on denatured collagen. Data are expressed as means ± SEM of migration indicated as a percentage of control (**A**, **B**, and **E**). $n = 3$ (**A**, **B**, and **E**). $^*P < 0.05$ compared with controls. CM, conditioned medium; NT, not treated.

found *in vivo*, following *in vitro* culture, our fibroblasts exhibited phosphorylated Erk and expressed α-SMA and platelet-derived growth factor receptor α, important markers of CAF-like stromal cells (data not shown). Therefore, we used these fibroblasts as a model of α-SMA–expressing stromal cells and examined whether blocking the HU177 epitope could alter growth factor–induced migration. Concentrated SKOV-3 CM and recombinant FGF-2 stimulation enhanced migration on denatured collagen (Figure 6, A and B). Importantly, addition of the anti-HU177 antibody to the migration wells significantly ($P < 0.05$) inhibited this growth factor–stimulated response, suggesting that not only can the HU177 epitope play a role in the basal cell migration but also that it can help regulate growth factor–mediated motility.

Previous studies have indicated that FGF-2 stimulation can initiate a complex signaling cascade, leading to the phosphorylation of multiple effector molecules and transcription factors, such as Erk1/2, which help coordinate the complex events required for cellular migration.[39–44] Given the known role of FGF-2 in regulating Erk activation, we examined the effects of blocking fibroblast interactions with the HU177 epitope on FGF-2–stimulated Erk phosphorylation. FGF-2 stimulated a small increase in Erk phosphorylation in cells attached to denatured collagen, whereas blocking the HU177 epitope reduced this phosphorylation (Figure 6C). A mean reduction in Erk phosphorylation from four independent experiments of approximately 40% was observed (Figure 6D). To confirm a role for MAP/Erk signaling in FGF-2–stimulated fibroblast motility on denatured collagen, migration assays were performed in the presence of a MEK inhibitor. Addition of the MEK inhibitor (PD98059) significantly ($P < 0.05$) blocked FGF-2–stimulated migration on denatured collagen, suggesting a role for MAP/Erk signaling in regulating this migratory response (Figure 6E).

Identification of Receptors for the HU177 Epitope

We previously identified the repetitive PGxPG-containing sequence as a critical component of the HU177 epitope.[15] In addition, other studies have indicated that antibodies directed to the HU177 epitope can bind to a variety of distinct PGxPG-containing sequences with different

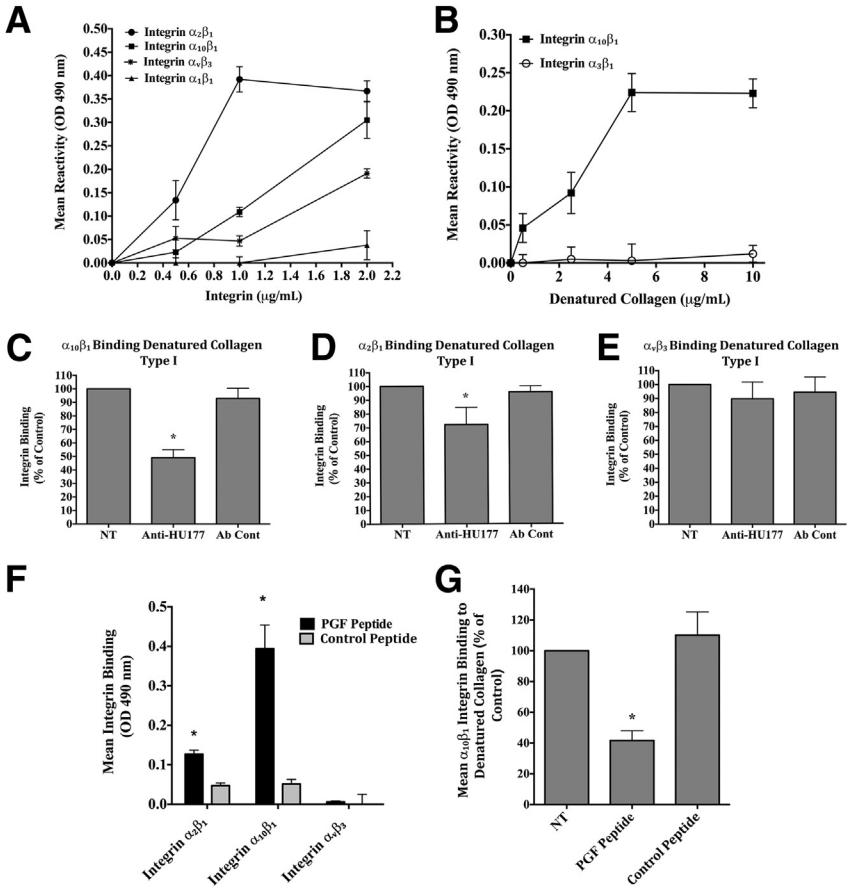

Figure 7 Integrin $\alpha_{10}\beta_1$ binds the HU177 collagen epitope. Wells were coated with denatured collagen (**A**, **C**–**E**), integrins $\alpha_{10}\beta_1$ and $\alpha_3\beta_1$ (**B**), or the synthetic HU177 epitope peptide or control peptide (**F**) and integrins (**A**, **C**–**E**) or denatured collagen (**B**) and allowed to bind. **A:** Integrin binding to denatured collagen. **B:** Binding of denatured collagen to immobilized integrins. **C:** Binding of $\alpha_{10}\beta_1$ to denatured collagen in the presence or absence of anti-HU177 or control antibodies (Ab Cont). **D:** Binding of $\alpha_2\beta_1$ to denatured collagen in the presence or absence of anti-HU177 or Ab Cont. **E:** Binding of $\alpha_v\beta_3$ to denatured collagen in the presence or absence of anti-HU177 or Ab Cont. **F:** Integrin binding to synthetic HU177 epitope or control peptide. **G:** Integrin binding to denatured collagen in the presence of synthetic HU177 epitope or control peptide. Experiments were completed at least three times. $^*P < 0.05$ compared with controls. NT, not treated; OD, optical density.

N-terminal and C-terminal flanking sequences found in collagen.[19] Given that a number of variations of this motif are found throughout collagen, it is possible that multiple receptors may have the ability to bind to these cryptic sites. To this end, integrin receptors are an important class of molecules known to mediate cellular interactions with ECM components and coordinate signaling cascades that govern cell motility. To define potential cell surface receptors for HU177 collagen epitope, we examined the ability of various recombinant integrins to bind denatured collagen. Integrin $\alpha_2\beta_1$ and $\alpha_v\beta_3$ dose-dependently bound denatured collagen, whereas $\alpha_1\beta_1$ caused minimal interactions (Figure 7A). Interestingly, integrin $\alpha_{10}\beta_1$, a collagen-binding receptor with a limited tissue distribution outside of cartilage,[45–48] also dose-dependently bound denatured collagen. To confirm $\alpha_{10}\beta_1$ binding to denatured collagen, we performed a second binding assay by immobilizing $\alpha_{10}\beta_1$ on microliter wells and examining soluble denatured collagen binding. Denatured collagen dose-dependently bound $\alpha_{10}\beta_1$ but not $\alpha_3\beta_1$ (Figure 7B). To identify which integrins capable of binding denatured collagen have the ability to bind the HU177 epitope, we examined the effects of blocking the HU177 epitope on integrin binding. Blocking the HU177 epitope inhibited $\alpha_{10}\beta_1$ binding by nearly 60% (Figure 7C), whereas $\alpha_2\beta_1$ binding was reduced by approximately 30% (Figure 7D). Binding of $\alpha_v\beta_3$ to denatured collagen was unaffected (Figure 7E). To confirm the integrin-binding specificity, direct binding to the synthetic PGxPG-containing HU177 epitope (PGF peptide) was performed. Although $\alpha_2\beta_1$ bound the HU177 epitope, $\alpha_{10}\beta_1$ exhibited fourfold greater binding, whereas $\alpha_v\beta_3$ failed to bind (Figure 7F). Moreover, the PGF peptide also partially competed binding of $\alpha_{10}\beta_1$ to denatured collagen by approximately 60% (Figure 7G). Taken together, these findings suggest that the little understood integrin $\alpha_{10}\beta_1$ can bind the HU177 collagen epitope.

Integrin $\alpha_{10}\beta_1$ Co-Localizes with α-SMA–Expressing Cells in Ovarian Tumors

Given our studies indicating the ability of $\alpha_{10}\beta_1$ to bind the HU177 epitope, we examined the expression of $\alpha_{10}\beta_1$ within ovarian tumors. $\alpha_{10}\beta_1$ was detected within human ovarian tumors and SKOV-3 tumors (Figure 8A). Expression of $\alpha_{10}\beta_1$ was associated predominately with α-SMA–positive cells as suggested by extensive co-localization (Figure 8B). Although minimal levels of α_{10} integrin protein (Figure 8C) and mRNA (data not shown) were detected in SKOV-3 cells, greater than fivefold higher levels were detected in α-SMA–expressing fibroblasts. We next examined the effects of blocking $\alpha_{10}\beta_1$ on fibroblast migration. Anti-α_{10} antibody inhibited FGF-2–stimulated migration on denatured collagen (Figure 8D). To confirm a role for $\alpha_{10}\beta_1$ integrin in fibroblast migration on denatured collagen, we knocked down

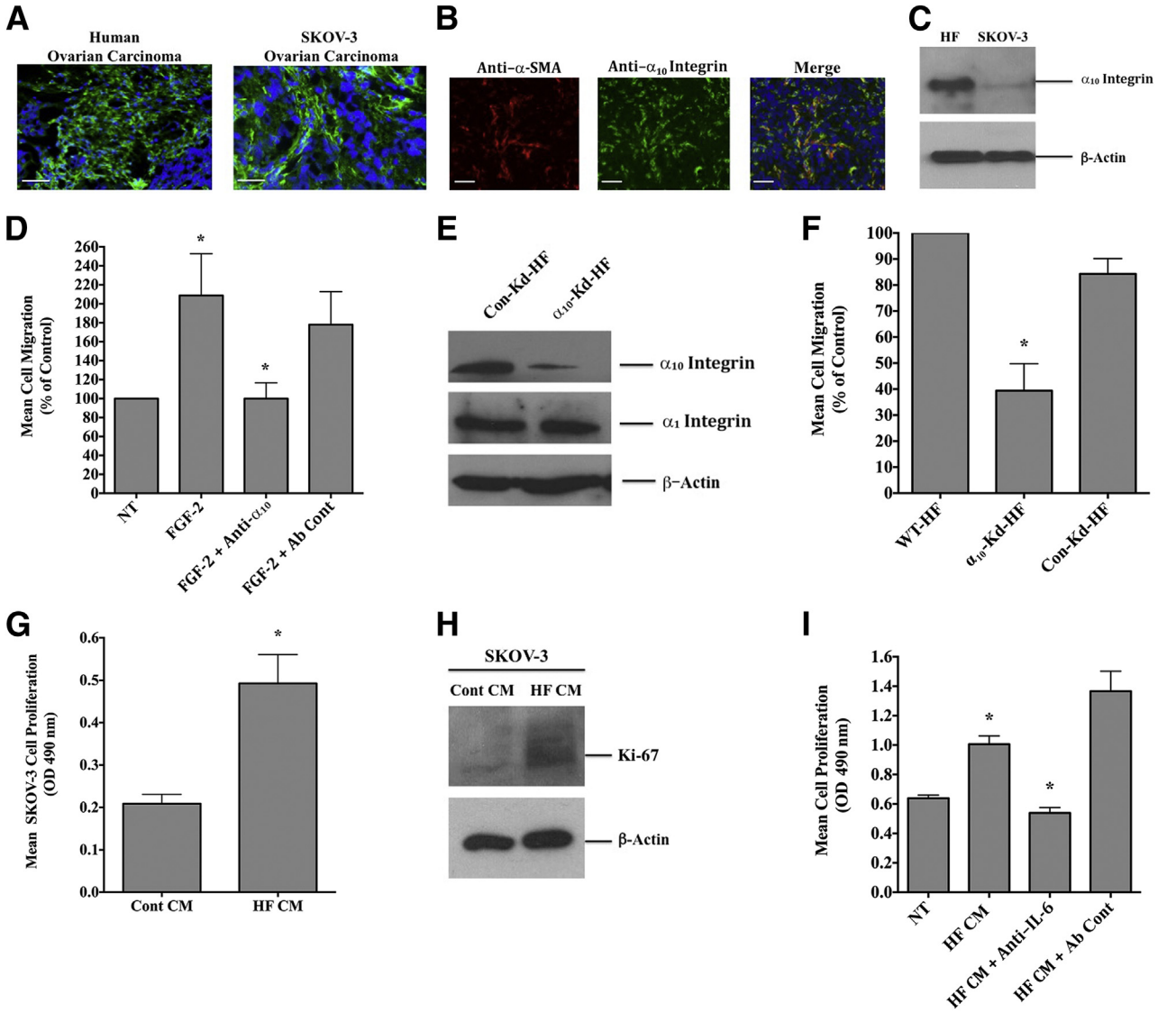

Figure 8 Expression and migratory function of $\alpha_{10}\beta_1$. **A:** Example of expression of $\alpha_{10}\beta_1$ (green) in human ovarian tumor biopsy specimen and SKOV-3 tumors. **B:** Example of co-expression of $\alpha_{10}\beta_1$ (green) and α-smooth muscle actin (α-SMA) (red)—expressing stromal cells within SKOV-3 tumors. **C:** Analysis of $\alpha_{10}\beta_1$ expression in SKOV-3 cells or fibroblasts (HF) by Western blot. **D:** Quantification of fibroblast growth factor (FGF)-2—induced fibroblasts migration in the presence or absence of anti-$\alpha_{10}\beta_1$ antibody or antibody control (Ab Cont). **E:** Western blot analysis of relative expression of α_{10} integrin, α_1 integrin, or β-actin in cell lysates from nonspecific control knockdown fibroblasts (Con-Kd-HF) or α_{10} integrin knockdown fibroblasts (α_{10}-Kd-HF). **F:** Quantification of FGF-2—induced migration of wild-type (WT-HF), α_{10} integrin knockdown fibroblasts (α_{10}-Kd-HF), or nonspecific control knockdown fibroblasts (Con-Kd-HF) on denatured collagen. **G:** SKOV-3 cell proliferation in the presence of control or fibroblast conditioned medium (CM). **H:** Western blot analysis for Ki-67 in lysates of SKOV-3 cells treated with fibroblast CM. **I:** SKOV-3 proliferation in the presence or absence of fibroblast CM and in the presence of anti—IL-6 or control antibodies. All experiments were completed at least three times with similar results. Data are expressed as means ± SEM. $n = 3$ (**D** and **F**). *$P < 0.05$ compared with controls. Scale bars = 63 μm. Original magnification, ×200 (**B**). NT, not treated.

expression $\alpha_{10}\beta_1$ integrin in these fibroblasts using α_{10}-specific shRNA. The relative levels of α_{10} protein were reduced by approximately 70%, whereas little change in α_1 integrin chain or actin was observed (Figure 8E). Next, we examined the ability of fibroblasts expressing altered levels of α_{10} integrin to migrate on denatured collagen. Although little if any change was observed in control transfected fibroblasts compared with wild-type parental cells, knocking down α_{10} integrin significantly ($P < 0.05$) inhibited fibroblast migration on denatured collagen by approximately 60% compared with controls (Figure 8F).

Given these results, it is possible that the reduction of α-SMA—positive stromal cells observed after anti-HU177 treatment leads to a reduction in an important source of protumorigenic cytokines that facilitate tumor growth and angiogenesis. To this end, we examined whether CM from α-SMA—expressing fibroblasts might contain soluble factors that enhance SKOV-3 cell growth. Fibroblast CM enhanced proliferation and Ki-67 antigen expression in SKOV-3 cells (Figure 8, G and H). These results are consistent with the ability of soluble factors released into the conditioned medium of these $\alpha_{10}\beta_1$-expressing fibroblasts to

enhance SKOV-3 tumor cell proliferation *in vitro*. To characterize potential protumorigenic factors expressed by these α-SMA−positive fibroblasts, concentrated serum free CM was screened using a multianalyte cytokine array for expression of 12 different cytokines. Among the cytokines that were expressed at the highest levels was IL-6 (Supplemental Table S1). Interestingly, IL-6 enhances growth of ovarian carcinoma cells[49,50]; thus, we examined whether this protumorigenic cytokine played a functional role in mediating the ability of α-SMA−expressing fibroblast CM to stimulate proliferation of SKOV-3 tumor cells. Fibroblast CM significantly enhanced SKOV-3 tumor cell proliferation, and a function-blocking antibody directed to IL-6 inhibited this response (Figure 8I). These data are consistent with a role for IL-6 expression from fibroblasts in promoting SKOV-3 tumor cell growth. Taken together, these findings suggest the possibility that α-SMA−expressing fibroblasts may serve as an important source of protumorigenic factors that facilitate SKOV-3 tumor growth and that selectively reducing accumulation of α-SMA−expressing stromal cells by inhibiting the interactions of these cells with the HU177 collagen epitope may contribute to the potent antitumor activity observed *in vivo*.

Discussion

The array of mechanisms by which stromal cells, such as endothelial cells and activated α-SMA−expressing fibroblasts, govern the malignant phenotype are diverse and include providing proteolytic enzymes that alter the biomechanical properties of ECM; the release of protumorigenic factors that act on both tumor and other cell types to alter their growth, survival, and migratory behavior; and the release of molecules that influence the host immune response.[1−6,51,52] Thus, selectively blocking the accumulation of protumorigenic stromal cells in malignant lesions likely represents an important therapeutic strategy. Although targeting stromal cells may provide a complementary strategy for tumor therapy, it remains challenging to selectively target them without disrupting their activity in normal tissues. The ECM represents an active control point for multiple mechanisms critical for regulating stromal cell behaviors, ranging from migration and proliferation to gene expression.[14] Therefore, inhibiting stromal cell−ECM interaction that selectively limits the accumulation of protumorigenic stromal cells in malignant lesions might represent a useful strategy to control tumor progression.

We found that the HU177 collagen epitope is abundantly generated within ovarian carcinomas compared with benign ovarian lesions. Importantly, previous studies have indicated that proteolytic enzymes, such as matrix metalloproteinase, can contribute to generation of the HU177 epitope *in vivo*.[16] We provide evidence that this cryptic collagen epitope played a role in SKOV-3 tumor growth, and these findings are consistent with a clinical trial that assessed tolerability and toxicity of mAb D93/TRC093.[20] Results of this study suggested no dose-limiting toxic effects and evidence of antitumor activity because a patient with an ovarian cancer had a reduction in metastatic liver lesions.[20] Although all cancers eventually progressed, 26% of patients had disease stabilization, and a patient with hemangiopericytoma, a tumor known to be highly infiltrated with stromal cells, had stable disease for nearly a year.[20]

Consistent with previous findings[15,18] the anti-HU177 antibody inhibited tumor-associated angiogenesis. These data are in agreement with previous studies that indicate that targeting the HU177 epitope could selectively inhibit endothelial cell adhesion and migration on denatured collagen, inhibit proliferation, up-regulate expression of P27KIP1, and inhibit angiogenesis *in vivo*.[15] Surprisingly, our new studies now indicate that targeting the HU177 epitope can also reduce the accumulation of α-SMA−expressing stromal cells within SKOV-3 tumors. Targeting the HU177 epitope inhibited SKOV-3 and α-SMA−expressing fibroblast adhesion and migration on denatured but not intact collagen, thereby specifically limiting the effect of this therapeutic agent to those tissues that express the HU177 epitope. FGF-2−induced fibroblast migration on denatured collagen was dependent in part on MAP/Erk signaling because inhibition of MAP/Erk signaling blocked this migratory response.

Cell migration is governed by a complex and integrated set of signaling events that are coordinated in part by the unique composition and integrity of the local ECM. However, the mechanisms by which cells sense the structural changes in the integrity of a given ECM environment during tumor growth to facilitate cellular motility induced by growth factors are not completely understood. In fact, inappropriate and/or enhanced migration may contribute to tumor cell invasion and metastasis as well as the accumulation of CAF-like stromal cells that contribute to tumor progression. Integrin-mediated interactions with ECM proteins are known to initiate assembly of multiple-protein complexes that coordinately regulate downstream signaling cascades, including Shc/Grab2/Ras and Fak/Src/Rap1 pathways that can activate MAPK/Erk signaling.[41] Our novel finding suggests that FGF-2 can enhance the phosphorylation of Erk in $\alpha_{10}\beta_1$-expressing fibroblasts and a function-blocking antibody directed to the HU177 cryptic collagen epitope inhibited Erk phosphorylation. Given that MAPK/Erk signaling plays a role in the ability of $\alpha_{10}\beta_1$-expressing fibroblasts to migrate on denatured collagen and the fact that denatured collagen selectively generates within the tumor microenvironment,[12,13,15,18] it would be interesting to speculate that the selective generation of the HU177 epitope within the ovarian tumor microenvironment may help facilitate enhanced activation of Erk, which may promote stromal cell migration and subsequent accumulation in tumors. Although multiple protein kinases contribute to the phosphorylation of Erk, the precise molecular mechanism by which cellular interactions with the HU177 epitope regulates FGF-2−induced activation of Erk is not known. Studies are currently under way to

define which kinases and/or phosphatases might contribute to the FGF-2–mediated regulation of Erk after interactions with the HU177 collagen epitope.

Given the reduction in α-SMA–expressing cells in tumors treated with anti-HU177 antagonists, selectively inhibiting migration of this population of stromal cells may limit a major cellular source of protumorigenic factors that play multiple roles in facilitating tumor cell survival and proliferation *in vivo*. In this regard, fibroblasts are known to express many protumorigenic factors, including IL-6, which has been previously found to enhance proliferation of ovarian carcinoma cells.[38,49,50] Consistent with these findings, our studies suggest that blocking IL-6 inhibited fibroblast CM-induced SKOV-3 cell growth. Given these findings and the high levels of IL-6 expressed by fibroblasts, our data are consistent with a mechanism by which targeting the HU177 epitope selectively limits accumulation of α-SMA fibroblasts, thereby reducing an important source of protumorigenic factors that enhance angiogenesis and tumor growth.

We provide new evidence that the little understood integrin $\alpha_{10}\beta_1$ functions as a receptor for the HU177 collagen epitope in fibroblasts. Given the variations within the HU177 PGxPG consensus site and the possibility of unique geometrical configurations and distinct flanking amino acid sequences found *in vivo*, it is possible that additional receptors may also recognize the HU177 epitope. Interestingly, little is known about the functions of $\alpha_{10}\beta_1$ outside chondrocyte and growth plate development.[45–48] However, α_{10} mRNA has been detected in murine heart, muscle tissues, and endothelial cells.[45–48] Studies suggest that FGF-2 stimulation of mesenchymal stem cells leads to up-regulation of α_{10}.[53] Moreover, mesenchymal stem cells have also been implicated as potential sources of α-SMA–expressing CAF-like cells in tumors.[54] In addition, studies now suggest enhanced expression of $\alpha_{10}\beta_1$ in melanoma cell lines compared with primary melanocytes and inhibiting $\alpha_{10}\beta_1$ in these cells resulted in a reduced migration.[55]

Given the ability of $\alpha_{10}\beta_1$ to bind the HU177 epitope, our data agree with a novel mechanism by which generation of the HU177 epitope provides a previously unrecognized ligand for $\alpha_{10}\beta_1$-expressing stromal cells that facilitates FGF-2–induced activation of Erk and subsequently the accumulation of α-SMA–positive stromal cells in ovarian tumors. In turn, the selective reduction in accumulation of this cell population by anti-HU177 antibody, in conjunction with its previously described antiangiogenic effects, likely contributes to its potent antitumor activity. Taken together, our findings provide new cellular and molecular insight into the roles of the HU177 cryptic epitope in ovarian tumor growth and provide new mechanistic understanding of the therapeutic effect observed in humans treated with mAb D93/TRC093.[20]

Supplemental Data

Supplemental material for this article can be found at *http://dx.doi.org/10.1016/j.ajpath.2016.01.015*.

References

1. Mursap N, Diamandis EP: Revisiting the complexity of the ovarian cancer microenvironment-clinical implications for treatment strategies. Mol Cancer Res 2012, 10:1254–1264
2. Schauer IG, Sood AK, Mok A, Liu J: Cancer associated fibroblasts and their putative role in potentiating the initiation and development of epithelial ovarian cancer. Neoplasia 2011, 13:393–405
3. Hanahan D, Coussens LM: Accessories to the crime: functions of cells recruited to the tumor microenvironment. Cancer Cell 2012, 21: 309–421
4. Qian BZ, Pollard JW: Macrophage diversity enhances tumor progression and metastasis. Cell 2010, 141:39–51
5. Bansai R, Tomar T, Ostman A, Poelstra K, Prakash J: Selective targeting of interferon γ to stromal fibroblasts and pericytes as a novel therapeutic approach to inhibit angiogenesis and tumor growth. Mol Cancer Ther 2012, 11:2419–2428
6. Mitra AK, Zillhardt M, Hua Y, Tiwari P, Murmann AE, Peter ME, Lengyel E: MicroRNAs reprogram normal fibroblasts into cancer-associated fibroblast in ovarian cancer. Cancer Discov 2012, 2: 1100–1108
7. Yao Q, Qu X, Yang Q, Mingqian W, Kong B: CLIC4 mediates TGF-β1-induced fibroblast-to-myofibroblast trans differentiation in ovarian cancer. Oncol Rep 2009, 22:541–548
8. Crawford Y, Kasman I, Yu L, Zhong C, Wu X, Modrusan Z, Kaminker J, Ferrara N: PDGF-C mediates the angiogenic and tumorigenic properties of fibroblasts associated with tumors refractory to anti-VEGF treatment. Cancer Cell 2009, 15:21–34
9. Ricciardelli C, Rodgers RJ: Extracellular matrix of ovarian tumors. Semin Reprod Med 2006, 24:270–282
10. Capo-Chichi CD, Smith ER, Yang DH, Roland IH, Vanderveer L, Hamiliton TC, Godwin AK, Xu XX: Dynamic alterations of the extracellular matrix environment of ovarian surface epithelial cells in premalignant transformation, tumorigenicity, and metastasis. Cancer 2002, 95:1802–1815
11. Akalu A, Roth JM, Caunt M, Policarpio D, Liebes L, Brooks PC: Inhibition of angiogenesis and tumor metastasis by targeting a matrix immobilized cryptic extracellular matrix epitope in laminin. Cancer Res 2007, 67:4353–4363
12. Hangai M, Kitaya N, Xu J, Chan CK, Kim JJ, Werb Z, Ryan SJ, Brooks PC: Matrix metalloproteinase-9-dependent exposure of a cryptic migratory control site in collagen is required before retinal angiogenesis. Am J Pathol 2002, 161:1429–1437
13. Xu J, Rodriguez D, Petitclerc E, Kim JJ, Hangai M, Yuen SM, Davis GE, Brooks PC: Proteolytic exposure of a cryptic site within collagen type-IV is required for angiogenesis and tumor growth in vivo. J Cell Biol 2001, 154:1069–1079
14. Cretu A, Brooks PC: Impact of the non-cellular microenvironment on metastasis: potential therapeutic and imaging opportunities. J Cell Physiol 2007, 213:391–402
15. Cretu A, Roth JM, Caunt M, Policarpio D, Formenti S, Gange P, Liebes L, Brooks PC: Disruption of endothelial cell interactions with the novel HU177 cryptic collagen epitope inhibits angiogenesis. Clin Cancer Res 2007, 13:3068–3078
16. Gagne PJ, Tihonov N, Li X, Glaser J, Qiao J, Silberstein M, Yee H, Gagne E, Brooks PC: Temporal exposure of cryptic collagen epitopes within ischemic muscle during hindlimb reperfusion. Am J Pathol 2005, 167:1349–1359
17. Ames JJ, Vary CPH, Brooks PC: Signaling pathways and molecular mediators in metastasis. Biomechanical ECM Switches and Tumor Metastasis. Springer Press 2012, 3:71–89
18. Pernasetti F, Nickel J, Clark D, Baeurle PA, Van Epps D, Freimark B: Novel anti-denatured collagen humanized antibody D93 inhibits angiogenesis and tumor growth: an extracellular matrix-based therapeutic approach. Int J Oncol 2006, 29:1371–1379
19. Freimark B, Clark D, Pernasetti F, Kickel J, Myszka D, Baeuerle PA, van Epps D: Targeting of humanized antibody D93 to sites of

angiogenesis and tumor growth by binding to multiple epitopes on denatured collagens. Mol Immunol 2007, 44:3741–3750
20. Robert F, Gordon MS, Rosen LS, Mendelson DS, Mulay M, Adams BJ, Alvare D, Theuer CP, Leigh BR: Final results from a phase I study of TRC093 (humanized anti-cleaved collagen antibody) in patients with solid cancer. Annual meeting proceedings, 2010, ASCO. Abstract No 3038.
21. Romero I, Bast RC: Minireview: human ovarian cancer: biology, current management, and paths to personalized therapy. Endocrinol 2012, 154:1593–1602
22. Vaughan S, Coward JI, Bast RC, Berchuck A, Berek JS, Brenton JD, Coukos G, Crum CC, Drapkin R, Etemadmoghadam D, Friedlander M, Gabra H, Kaye SB, Lord CJ, Lengyel E, Levine DA, McNeish IA, Menon U, Mills GB, Nephew KP, Oza AM, Sood AK, Stronach EA, Walczak H, Bowtell DD, Balkwill FR: Rethinking ovarian cancer: recommendations for improving outcomes. Nat Rev Cancer 2011, 11:719–725
23. Kuman RJ, Shih M: The origin and pathogenesis of epithelial ovarian cancer: a proposed unifying theory. Am J Surg Pathol 2010, 34: 433–443
24. Kim J, Coffey DM, Creighton CJ, Yu Z, Hawkins SM: High-grade serous ovarian cancer arises from fallopian tube in a mouse model. Proc Natl Acad Sci U S A 2012, 109:3921–3926
25. Ozols RF, Bookman MA, Connolly DC, Daly MB, Godwin AK, Schilder RJ, Xu X, Hamilton TC: Focus on epithelial ovarian cancer. Cancer Cell 2004, 5:19–24
26. Granot D, Addadi Y, Kalchenko V, Harmelin A, Kunz-Schugart LA, Neeman M: In vivo imaging of systemic recruitment of fibroblasts to the angiogenic rim of ovarian carcinoma tumors. Cancer Res 2007, 67:9180–9190
27. Cai J, Tang H, Xu L, Wang X, Yang C, Ruan S, Guo J, Hu S, Wang Z: Fibroblasts in omentum activated by tumor cells promote ovarian cancer growth, adhesion and invasiveness. Carcinogenesis 2013, 33:20–29
28. Ko SY, Barengo N, Ladanyi A, Lee JS, Marini F, Lengyel E, Naora H: HoxA9 promotes ovarian cancer growth by stimulating cancer-associated fibroblasts. J Clin Invest 2012, 122:3603–3617
29. Roth JM, Zelmanovich A, Policarpio D, Ng B, MacDonald S, Formenti S, Liebes L, Brooks PC: Recombinant α2(IV) NC1 domain inhibits tumor cell-extracellular matrix interactions, induces cellular senescence, and inhibits tumor growth in vivo. Am J Pathol 2005, 166:901–911
30. Brooks PC, Montgomery AM, Rosenfeld M, Reisfeld RA, Hu T, Klier G, Cheresh DA: Integrin αvβ3 antagonists promote tumor regression by inducing apoptosis of angiogenic blood vessels. Cell 1994, 79:1157–1164
31. Zhu GG, Melkko J, Risteli J, Kauppila A, Risteli L: Differential processing of collagen type-I and type III procollagens in the tumor cysts and peritoneal ascites fluid of patients with benign and malignant ovarian tumors. Clin Chim Acta 1994, 229:87–97
32. Santala M, Risteli J, Risteli L, Pulstola U, Kacinski BM, Stanley ER, Kauppila A: Synthesis and breakdown of fibrillar collagens: concomitant phenomena in ovarian cancer. Br J Cancer 1998, 77: 1825–1831
33. Kawamura K, Komohara Y, Takaishi K, Katabuchi H, Takeya M: Detection of M2 macrophages and colony stimulating factor 1 expression in serous and mucinous ovarian epithelial tumors. Pathol Int 2009, 59:300–305
34. Cubillos-Ruiz JR, Rutkowski M, Conejo-Garcia JR: Blocking ovarian cancer progression by targeting tumor microenvironmental leukocytes. Cell Cycle 2010, 9:260–268
35. Petitclerc E, Stromblad S, von Schalscha TL, Mitjans F, Piulats J, Montgomery AM, Cheresh DA, Brooks PC: Integrin $\alpha_v\beta_3$ promotes M21 melanoma growth in human skin by regulating tumor cell survival. Cancer Res 1999, 59:2724–2730
36. Anderberg C, Pietras K: On the origin of cancer-associated fibroblasts. Cell Cycle 2009, 8:1461–1465
37. Erez N, Truitt M, Olsen P, Hanahan D: Cancer-associated fibroblasts are activated in incipient neoplasia to orchestrate tumor-promoting inflammation in an NFκb-dependent manner. Cancer Cell 2010, 17: 135–147
38. Erez N, Glanz S, Raz Y, Avivi C, Barshack I: Cancer associated fibroblasts express pro-inflammatory factors in human breast and ovarian tumors. Biochem Biophys Res Commun 2013, 437:397–402
39. Cunningham DL, Sweet SMM, Cooper HJ, Heath JK: Differential phosphoproteomics of fibroblast growth factor signaling: identification of Src family kinase-mediated phosphorylation events. J Proteome Res 2010, 9:2317–2328
40. Kanda S, Miyata Y, Kanetake H, Smithgall TE: Fibroblast growth factor-2 induces the activation of Src through Fes, which regulates focal adhesion disassembly. Exp Cell Res 2006, 312:3015–3022
41. Barberis L, Wary KK, Fiucci G, Liu F, Hirsch E, Brancaccio M, Altruda F, Tarone G, Giancotti FG: Distinct roles of the adaptor protein Shc and focal adhesion kinase in integrin signaling to Erk. J Biol Chem 2000, 275:36532–36540
42. Cho AY, Klemke RL: Extracellular-regulated kinase activation and CAS/Crk coupling regulate cell migration and suppress apoptosis during invasion of the extracellular matrix. J Cell Biol 2000, 149:223–236
43. Kottakis F, Polytarchou C, Foltopoulou P, Sanidas I, Kampranis SC, Tsichlis PN: FGF-2 regulates cell proliferation, migration and angiogenesis through an NDY1/KDM2B-miR-101-EZH2 pathway. Mol Cell 2011, 43:285–298
44. Boilly B, Vercoutter-Edouart AS, Hondermarck H, Nurcombe V, Bourhis XL: FGF signals for cell proliferation and migration through different pathways. Cytokine Growth Factor Rev 2000, 11:295–302
45. Lehnert K, Ni J, Leung E, Gough S, Morris CM, Liu D, Wang SX, Langley R, Krissansen GW: The integrin α_{10} subunit: expression pattern, partial gene structure, and chromosomal localization. Cytogent Cell Genet 1998, 87:238–244
46. Bengtsson T, Camper L, Schneller M, Lundgren-Akerlund E: Characterization of the mouse integrin subunit α_{10} gene and comparison with its human homologue genomic structure, chromosomal localization and identification of splice variants. Matrix Biol 2001, 20:565–576
47. Bengtsson T, Aszodi A, Nicolae C, Hunziker EB, Lundgren-Akerlund E, Fassler R: Loss of $\alpha_{10}\beta_1$ integrin expression leads to moderate dysfunction of growth plate chondrocytes. J Cell Sci 2004, 118:929–936
48. Camper L, Holmvall K, Wangnerd C, Asodi A, Lundgren-Akerlund E: Distribution of the collagen-binding integrin $\alpha_{10}\beta_1$ during mouse development. Cell Tissue Res 2001, 306:107–116
49. Wang Y, Li L, Jin X, Sun W, Zhang X, Xu RC: Interleukin-6 signaling regulates anchorage-independent growth, proliferation, adhesion and invasion in human ovarian cancer cells. Cytokine 2012, 59:228–236
50. Wang Y, Xu RC, Zhang XL, Niu XL, Qu Y, Li LZ, Meng XY: Interleukine-8 secretion by ovarian cancer cells increases anchorage-independent growth, proliferation, angiogenic potential, adhesion and invasion. Cytokine 2012, 59:145–155
51. Santos AM, Jung J, Aziz N, Kissil JL, Pure E: Targeting fibroblast activation protein inhibits tumor stromagenesis and growth in mice. J Clin Invest 2009, 119:3613–3625
52. Kraman M, Bambrough PJ, Arnold JN, Roberts EW, Magiera L, Jones JO, Gopinathan A, Tuveson DA, Fearon DT: Suppression of anti-tumor immunity by stromal cells expressing fibroblast activation protein-α. Science 2001, 250:827–830
53. Varas L, Ohlsson LB, Honeth G, Olsson A, Bengtsson T, Wiberg C, Bockermann R, Järnum S, Richter J, Pennington D, Johnstone B, Lundgren-Akerlund E, Kjellman C: α_{10} integrin expression is upregulated on fibroblast growth factor-2-treated mesenchymal stem cells with improved chondrogenic differential potential. Stem Cell Develop 2007, 16:965–978
54. Mishra PJ, Mishra PJ, Glod JW, Banerjee D: Mesenchymal stem cells: flip side of the coin. Cancer Res 2009, 69:1255–1258
55. Wenke AK, Kjellman C, Lundgren-Akerlund E, Uhlmann C, Haass NK, Herlyn M, Bosserhoff AK: Expression of integrin α_{10} is induced in malignant melanoma. Cell Oncol 2007, 29:373–386